

Unlock your experimental potential
with power and agility
BD FACSymphony™ A5 SE Cell Analyzer
Discover the difference >



Macrophages Switch Their Phenotype by Regulating Maf Expression during Different Phases of Inflammation

This information is current as
of February 26, 2022.

Kenta Kikuchi, Mayumi Iida, Naoki Ikeda, Shigetaka
Moriyama, Michito Hamada, Satoru Takahashi, Hiroshi
Kitamura, Takashi Watanabe, Yoshinori Hasegawa, Koji
Hase, Takeshi Fukuhara, Hideyo Sato, Eri H. Kobayashi,
Takafumi Suzuki, Masayuki Yamamoto, Masato Tanaka and
Kenichi Asano

J Immunol 2018; 201:635-651; Prepublished online 15 June
2018;

doi: 10.4049/jimmunol.1800040

<http://www.jimmunol.org/content/201/2/635>

**Supplementary
Material** <http://www.jimmunol.org/content/suppl/2018/06/14/jimmunol.1800040.DCSupplemental>

References This article **cites 75 articles**, 24 of which you can access for free at:
<http://www.jimmunol.org/content/201/2/635.full#ref-list-1>

Why *The JI*? Submit online.

- **Rapid Reviews! 30 days*** from submission to initial decision
- **No Triage!** Every submission reviewed by practicing scientists
- **Fast Publication!** 4 weeks from acceptance to publication

**average*

Subscription Information about subscribing to *The Journal of Immunology* is online at:
<http://jimmunol.org/subscription>

Permissions Submit copyright permission requests at:
<http://www.aai.org/About/Publications/JI/copyright.html>

Email Alerts Receive free email-alerts when new articles cite this article. Sign up at:
<http://jimmunol.org/alerts>

The Journal of Immunology is published twice each month by
The American Association of Immunologists, Inc.,
1451 Rockville Pike, Suite 650, Rockville, MD 20852
Copyright © 2018 by The American Association of
Immunologists, Inc. All rights reserved.
Print ISSN: 0022-1767 Online ISSN: 1550-6606.



Macrophages Switch Their Phenotype by Regulating Maf Expression during Different Phases of Inflammation

Kenta Kikuchi,* Mayumi Iida,* Naoki Ikeda,* Shigetaka Moriyama,* Michito Hamada,[†] Satoru Takahashi,[†] Hiroshi Kitamura,[‡] Takashi Watanabe,[§] Yoshinori Hasegawa,[¶] Koji Hase,^{||} Takeshi Fukuhara,^{#,**} Hideyo Sato,^{††} Eri H. Kobayashi,^{‡‡} Takafumi Suzuki,^{‡‡} Masayuki Yamamoto,^{‡‡} Masato Tanaka,* and Kenichi Asano*

Macrophages manifest distinct phenotype according to the organs in which they reside. In addition, they flexibly switch their character in adaptation to the changing environment. However, the molecular basis that explains the conversion of the macrophage phenotype has so far been unexplored. We find that CD169⁺ macrophages change their phenotype by regulating the level of a transcription factor Maf both in vitro and in vivo in C57BL/6J mice. When CD169⁺ macrophages were exposed to bacterial components, they expressed an array of acute inflammatory response genes in Maf-dependent manner and simultaneously start to downregulate Maf. This Maf suppression is dependent on accelerated degradation through proteasome pathway and microRNA-mediated silencing. The downregulation of Maf unlocks the NF-E2-related factor 2-dominant, cytoprotective/antioxidative program in the same macrophages. The present study provides new insights into the previously unanswered question of how macrophages initiate proinflammatory responses while retaining their capacity to repair injured tissues during inflammation. *The Journal of Immunology*, 2018, 201: 635–651.

Tissue macrophages are characterized by their remarkable heterogeneity and versatility. A considerable amount of effort has been paid to classifying macrophages according to their anatomic location, origin, and surface markers (1–4). Recently, novel approaches to characterizing tissue macrophages on the basis of the expression pattern of cell type-specific transcription factors have been proposed. For example, GATA6 is selectively expressed in peritoneal macrophages and supports the expression of subpopulation-specific gene clusters in these cells (5). In the spleen, Spi-C is highly expressed in red pulp macrophages but not in monocytes or dendritic cells (DCs). Its deficiency impairs the efficient phagocytosis of RBCs by red pulp macrophages (6). These studies illustrate the critical role of cell

type-specific transcription factors in the differentiation and/or polarization of tissue macrophages.

Acute inflammation is a beneficial host response directed toward foreign Ags or tissue injury. However, in the late phase of inflammation, the program should be converted to one that promotes tissue repair and regeneration. It is now determined that tissue macrophages play a pivotal role in this process by switching their phenotype during the different phases of inflammation (7, 8). For example, in a model of liver injury and subsequent fibrosis, Ly-6C^{hi} inflammatory monocytes undergo phenotypic conversion to cells exhibiting a tissue-reparative phenotype (9). The initial influx of monocyte-derived macrophages aggravates ischemia-induced kidney injury, but the in situ proliferation and differentiation of these macrophages during the recovery phase from injury is

*Laboratory of Immune Regulation, The School of Life Sciences, Tokyo University of Pharmacy and Life Sciences, Tokyo 192-0392, Japan; [†]Department of Anatomy and Embryology, Faculty of Medicine, University of Tsukuba, Tsukuba 305-8575, Japan; [‡]Laboratory of Veterinary Physiology, Department of Veterinary Medicine, School of Veterinary Medicine, Rakuno Gakuen University, Ebetsu 069-8501, Japan; [§]Laboratory for Integrative Genomics, RIKEN Center for Integrative Medical Sciences, Yokohama 230-0045, Japan; [¶]Department of Research and Development, Kazusa DNA Research Institute, Kisarazu 292-0818, Japan; ^{||}Division of Biochemistry, Graduate School of Pharmaceutical Sciences, Keio University, Tokyo 105-8512, Japan; [#]Department of Neurology, Juntendo University Graduate School of Medicine, Tokyo 113-8421, Japan; ^{**}Laboratory of Oncology, The School of Life Sciences, Tokyo University of Pharmacy and Life Sciences, Tokyo 192-0392, Japan; ^{††}Department of Medical Technology, Faculty of Medicine, Niigata University, Niigata 951-8518, Japan; and ^{‡‡}Department of Medical Biochemistry, Tohoku University Graduate School of Medicine, Sendai 980-8575, Japan

ORCID: 0000-0002-6084-7559 (K.K.); 0000-0002-8540-7760 (S.T.); 0000-0001-9643-3211 (H.K.); 0000-0002-6184-0375 (T.W.); 0000-0003-2904-6611 (Y.H.); 0000-0003-2950-9516 (T.F.); 0000-0002-5568-0731 (E.H.K.).

Received for publication January 10, 2018. Accepted for publication April 30, 2018.

This work was supported by a Grant-in-Aid for Scientific Research (B) (26293089) and a Grant-in-Aid for Scientific Research (C) (26460401) from the Japan Society for the Promotion of Science, a Grant-in-Aid for Scientific Research on Innovative Areas (Homeostatic Regulation by Various Types of Cell Death) (26110006) from the Ministry of Education, Culture, Sports, Science and Technology (MEXT) in Japan, the MEXT-Supported Program for the Strategic Research Foundation at Private Universities (2014–2019) in Japan, the Daiichi-Sankyo Foundation, the Uehara Memorial Foundation, the Takeda Science Foundation, and the Naito Foundation.

K.K. performed the majority of experiments with help from M.I., S.M., N.I., and K.A. and was involved in study design. S.M. interpreted microarray analysis data. N.I. and M.I. constructed retrovirus vectors. M.H. and S.T. provided Maf-deficient mice and were involved in study design. H.K. and T.W. performed microarray analysis. Y.H. performed microRNA sequencing analysis. K.H. provided germ-free mice. T.F. provided Rosa26-CAG-LSL-tandem Tomato mice. H.S. provided xCT reporter plasmid. E.H.K., T.S., and M.Y. provided NF-E2-related factor 2-deficient mice and were involved in study design. M.T. and K.A. contributed to study design and figure preparation and wrote the manuscript. All authors contributed to data analysis and revised the manuscript.

Address correspondence and reprint requests to Prof. Masato Tanaka and Dr. Kenichi Asano, Tokyo University of Pharmacy and Life Sciences, 1432-1 Horinouchi, Hachioji, Tokyo 192-0392, Japan. E-mail addresses: mtanaka@toyaku.ac.jp (M.T.) and asanok@toyaku.ac.jp (K.A.)

The online version of this article contains supplemental material.

Abbreviations used in this article: 7AAD, 7-aminoactinomycin D; ARE, antioxidant response element; BM, bone marrow; BMDC, BM-derived DC; BMDM, BM-derived macrophage; DC, dendritic cell; DEM, diethyl maleate; DSS, dextran sodium sulfate; GF, germ-free; LN, lymph node; LP, lamina propria; MARE, Maf recognition element; MHC II, MHC class II; miR, microRNA; Nrf2, NF-E2-related factor 2; PB, peripheral blood; qRT-PCR, quantitative RT-PCR; tBHP, *tert*-butyl hydroperoxide; UTR, untranslated region; WT, wild-type.

Copyright © 2018 by The American Association of Immunologists, Inc. 0022-1767/18/\$35.00

beneficial for tubular repair (10). These findings highlight the plasticity of tissue macrophages as a critical determinant of inflammatory resolution; however, the molecular basis that enables their reversible adaptation to the changing environment has so far been unclarified.

CD169⁺ macrophages localize at the boundary between tissues and circulating fluids. They capture particulate materials such as dead cells (11–13), immune complexes (14), or viral particles (15) that flow into the tissue and maintain tolerance or activate surrounding immune cells. This line of evidence categorizes CD169⁺ cells as “perivascular sentinels” that survey the entry of particulate Ags in the circulating fluids (16) and suggests the presence of a differentiation program common to CD169⁺ macrophages residing in different organs. In our previous study, we identified a chemokine CCL8 as a signature for CD169⁺ macrophages in the colon. CCL8 is produced selectively by the CD169⁺ subsets of colon macrophages and exacerbates experimental colitis by recruiting inflammatory monocytes (17).

In this study, we used the colon CD169⁺ macrophages to identify transcription factors that regulate phenotypic conversion. We identified Maf as a key regulator of acute inflammatory responses in the bone marrow (BM)-derived macrophages (BMDMs) and the colon CD169⁺ macrophages. In the early stage of inflammation, Maf inhibits the conversion of CD169⁺ macrophages to cells with the tissue-protective phenotype by negatively regulating the downstream targets of another transcription factor, NF-E2-related factor 2 (Nrf2). Following acute inflammatory response, macrophages start to downregulate Maf both at a protein and an mRNA level. This suppression was a result of accelerated degradation through proteasome pathway and microRNA (miR)-mediated gene silencing. The repression of Maf paves the way for an Nrf2-dominant cytoprotective/antioxidative phenotype in these macrophages *in vivo*. Collectively, we provided evidence that Maf serves as a molecular switch that converts the macrophage phenotype during the early and late phases of inflammation.

Materials and Methods

Reagents

LPS from *Escherichia coli* (O55:B5) and *tert*-butyl hydroperoxide (tBHP) were purchased from Sigma-Aldrich. Mouse recombinant IFN- γ and IL-4 were from PeproTech. Diethyl maleate (DEM) was from Wako Pure Chemical. CDDO-Im was from R&D Systems. Cell Counting Kit was from Dojindo. MG132 was from Peptide Institute. miRCURY LNA miR mimics were from Exiqon. Lipofectamine 3000 and FuGENE 6 were from Thermo Fisher Scientific and Promega, respectively.

Animals

Six- to twelve-week-old CD45.2⁺ C57BL/6J female mice were purchased from CLEA Japan. C57BL/6N mice maintained in a germ-free (GF) condition were donated by K. Hase (Keio University) or purchased from CLEA Japan. Maf-deficient mice (18) and Nrf2-deficient mice (19) with C57BL/6 background have been described previously. CD169-Cre mice (20) were crossed with Rosa26-YFP mice (21) or Rosa26-CAG-LSL-tandem Tomato mice (The Jackson Laboratory) to generate CD169 fate-mapping mice. Specific pathogen-free mice were maintained in the animal facilities of Tokyo University of Pharmacy and Life Sciences. All experiments using mice were approved by the Tokyo University of Pharmacy and Life Sciences Animal Care Committee (L15-03, L16-14, L17-24, and L17-25) and performed in accordance with applicable guidelines and regulations.

Generation of chimeric mice

Fetal liver and BM chimeric mice were generated according to a previously reported protocol (22) with a slight modification. Recipient CD45.2⁺ C57BL/6J mice were exposed to a lethal dose of x-ray irradiation (8 Gy) to prevent recovery of endogenous hematopoietic cells. Three million liver cells from CD45.1⁺ Maf^{+/+} or Maf^{-/-} donor fetus (E14.5) were i.v. injected into irradiated CD45.2⁺ recipients. Five million BM cells from the primary fetal liver chimeric mice were transferred into irradiated CD45.2⁺ secondary recipients to generate

BM chimeric mice. Replacement of hematopoietic cells in the peripheral blood (PB) of the recipient mice was analyzed by flow cytometry 8 wk after the transplantation.

Preparation of BMDMs and BM-derived DCs

BM cells were cultured either in MEM α /10% FCS/10% M-CSF (CMG14-12 culture medium) or in RPMI 1640/10% FCS/10% GM-CSF (MGM-5 culture medium) to generate BMDMs or BM-derived DCs (BMDCs), respectively. Those cells were stimulated with 100 ng/ml LPS or 100 μ M DEM. In some experiments, BMDMs were pretreated with DEM for 5 h. After washing with medium, those cells were further stimulated with LPS for 19 h. For cell viability assay, BMDMs were treated with different concentrations of tBHP for 24 h. The viability was determined by Cell Counting Kit (Dojindo) according to the manufacturer's protocol. For the polarization of BMDMs to M1 or M2 activation states, BMDMs were stimulated either with medium alone, 10 ng/ml LPS and 20 ng/ml IFN- γ , or 20 ng/ml IL-4 for 24 h.

Plasmids

To construct the mouse *Ccl8* gene promoter-luciferase reporter plasmid (CCL8-pGL4), an ~0.3-kb DNA fragment of the mouse *Ccl8* gene promoter was amplified by PCR using mouse genomic DNA as template and the following primers: forward, 5'-ATA GGT ACC TTC ATT TCT ATG TTT CAG AAT CCC TG-3'; reverse, 5'-TAA TCT CGA GTG TTG AAG GCA AAG ATT TTG GAG TGA AG-3'. The amplified DNA fragment was digested with KpnI and XhoI and then subcloned into the pGL4.10 vector (Promega). The Maf recognition element (MARE) mutant reporter plasmid (CCL8 mut1-, mut2-, mut3-, or mut4-pGL4) was generated by site-directed mutagenesis using the following primer pairs: forward, 5'-CCA GTG GGA CTG CTT CCT CCA GAA GAG AGG TTT CAG ATG CTT GCC C-3'; reverse, 5'-GGG CAA GCA TCT GAA ACC TCT CTT CTG GAG GAA GCA GTC CCA CTG G-3'; forward, 5'-AGA TTT TAG CAT CTT ATT CTG AAG AGA CTG CCT TCC AGC TGC CGG GA-3'; reverse, 5'-TCC CGG CAG CTG GAA GCG AGT CTC TTC AGA ATA AGA TGC TAA AAT CT-3'; and forward, 5'-ATC TCA TGA TCT GAT GAC TAT CTC TTC TAA CAA AGA TCT TGC TTT CA-3'; reverse, 5'-TGA AAG CAA GAT CTT TGT TAG AAG AGA TAG TCA GAT CAT GAG AT-3'. To construct the mouse *Slpi* gene promoter-luciferase reporter plasmid (SLPI-pGL4), an ~0.8-kb DNA fragment of mouse *Slpi* gene promoter was amplified by PCR using the following primers: forward, 5'-AGC AGG TAC CAG GAC ACC ACA GCT CCA CGC-3'; reverse, 5'-TAA TCT CGA GCA GGG GAG CTC TGA CCA-3'. The PCR product was digested with KpnI and XhoI and cloned into pGL4.10 vector (Promega). The mouse *Slc7a11* gene promoter was cut out from pGL3-0.7 plasmid (23) to pGL4.17 vector (Promega) to generate xCT luciferase reporter plasmid (xCT-0.7-pGL4). To construct the Maf expression plasmid (Maf-BOS-EX), Maf cDNA (18) was subcloned into an EcoRI- and NheI-digested BOS-EX plasmid. To generate the Nrf2 expression plasmid (Nrf2-BOS-EX), Nrf2 cDNA was amplified by PCR using mouse genomic DNA as template and the following primers: forward, 5'-ATA GGT ACC CGC CCT CAG CAT GAT GGA CT-3'; reverse, 5'-GGC CGC TAG CCT AGT TTT TCT TTG TAT CTG-3'. The PCR product was digested with KpnI and NheI and then subcloned into BOS-EX plasmid. To construct the luciferase-Maf 3'-untranslated region (UTR) reporter plasmid (Maf 3'-UTR-psiCHECK2), an ~2.5-kbp DNA fragment of *Maf* 3'-UTR region was amplified by PCR using following primers: forward, 5'-GTC CGG AAT TCG ACG CCT ACA AGG AGA AAT ACG AG-3'; reverse, 5'-ATA AGA ATG CGG CCG TCA CGC GTG GTT AGT TAG TA-3'. PCR fragment was digested with EcoRI and NotI and then 2.2-kbp restriction fragment was cloned into the pBluescript II SK(+). The plasmid was digested with XhoI and NotI, and the restriction fragment was cloned into the downstream of *Renilla* luciferase cDNA of a psiCHECK2 Vector (Promega).

Retrovirus transfection

Puromycin resistance gene in a pMSCVpuro vector (TaKaRa Bio) was replaced by Venus cDNA using the GeneArt Seamless Cloning and Assembly Kit (Thermo Fisher Scientific) according to the manufacturer's protocol. The protruding ends of an EcoRV- and SacI-digested Maf cDNA (18) fragment were converted to blunting end with DNA Blunting Kit (TaKaRa Bio) and then ligated into an HpaI-digested Venus-pMSCV vector. Packaging cell line PLAT-E cells (24) were grown in culture flask (Corning) and transiently transfected with Maf-Venus-pMSCV (Maf retrovirus vector) or Venus-pMSCV (Empty retrovirus vector) using the FuGENE 6 Reagent (Promega) according to the manufacturer's protocol. Forty-eight hours after the transfection, the culture supernatant was harvested and filtrated through a 0.45- μ m pore syringe-driven filter unit (Millipore). BM cells (1.8×10^5 cells per well in a 48-well plate) were cultured in the

presence of GM-CSF for 2 d and then subjected to retrovirus infection using the polybrene. Sixteen hours postinfection, the medium was replaced with fresh medium, and the cells were cultured for 2 more days. Forty hours postinfection, BMDMs were stimulated with 100 ng/ml of LPS for 5 h. For the forced expression of Maf in BMDMs, BM cells were cultured in the presence of M-CSF. Those cells were seeded on a 48-well plate at the concentration of 5×10^4 cells per well on day 4. On the next day, BMDMs were subjected to retrovirus infection without using the polybrene. Forty hours postinfection, BMDMs were treated with or without 100 μ M DEM for 5 h, followed by stimulation with LPS for 19 h.

Enzymatic digestion of the lymph node

Lymph node (LN) macrophages and DCs were prepared as described previously (11). In short, peripheral LNs were digested with a mixture of Collagenase IIs (750 μ g/ml; Sigma-Aldrich) and DNase I (10 μ g/ml; Sigma-Aldrich) in $1 \times$ HBSS containing Ca^{2+} and Mg^{2+} for 25 min at 37°C.

Enzymatic digestion of the colon lamina propria

Colon lamina propria (LP) cells were prepared as described previously (17) with a slight modification. The entire colon was removed, flushed several times with PBS to remove feces, and opened longitudinally. Two- to three-centimeter pieces of colon were incubated in HBSS not containing Ca^{2+} or Mg^{2+} /2% FBS/20 mM EDTA (pH 7.2) for 15 min at 37°C. The tissue was washed in PBS to remove EDTA, and the residual epithelial layer was removed by gently sliding curved forceps. The tissue was minced into <5 mm-long pieces followed by digestion in RPMI 1640/2% FCS/150 μ g ml^{-1} Liberase TL/500 μ g ml^{-1} DNase I (Roche or Worthington)/1% Dispase (BD Biosciences)/10 mM HEPES (Nacalai)/1% penicillin and streptomycin (Wako Pure Chemical) for 40 min at 37°C.

Flow cytometry

For flow cytometric analysis, cells were preincubated with Fc blocker (clone: 2.4G2, 2.5 μ g ml^{-1} ; Tonbo Biosciences) and then stained with combinations of following Abs: anti-CD8a (clone: 53-6.7, 0.5 μ g ml^{-1}), anti-CD36 (clone: 72-1, 1.0 μ g ml^{-1}), anti-MHC class II (MHC II) (clone: M5/114, 0.3 μ g ml^{-1} ; eBioscience), anti-MHC class I (clone: AF6-88.5, 2 μ g ml^{-1} ; BD Biosciences), anti-CD3e (clone: 145-2C11, 2.0 μ g ml^{-1}), anti-CD11b (clone: M1/70, 0.5 μ g ml^{-1}), anti-CD11c (clone: N418, 1.25 μ g ml^{-1}), anti-CD19 (clone: 6D5, 2 μ g ml^{-1}), anti-CD45.2 (clone: 104, 2.0 μ g ml^{-1}), anti-CD64 (clone: X54-5/7, 2.0 μ g ml^{-1}), anti-CD115 (clone: AFS98, 2.0 μ g ml^{-1}), anti-CD206 (clone: C068C2, 2.0 μ g ml^{-1}), anti-F4/80 (clone: CI:A3-1, 2.0 μ g ml^{-1}), anti-Ly-6C (clone: HK1.4, 0.8 μ g ml^{-1}), anti-Ly-6G (clone: 1A8, 2.0 μ g ml^{-1}), anti-Siglec F (clone: E50-2440, 2.0 μ g ml^{-1} ; BioLegend), biotinylated anti-CD169 [clone: M7, 4 μ g ml^{-1} generated and biotinylated in our laboratory (17)], anti-CD204 (clone: REA148, $\times 10$; Miltenyi), or anti-CD45.1 (clone: A20, 2.5 μ g ml^{-1} ; BioLegend or Tonbo Biosciences). Biotinylated rat IgG2b (clone: RTK4530, 4 μ g ml^{-1} ; BioLegend) or REA Control (clone: REA293, $\times 10$; Miltenyi) was used as an isotype control for biotinylated anti-CD169 or anti-CD204, respectively. Alexa Fluor 488 streptavidin (Invitrogen) or PE streptavidin (BioLegend) was used to detect biotinylated Abs. We used 7-aminoactinomycin D (7AAD) (Tonbo Biosciences or BioLegend) or DAPI (Dojindo) to exclude dead cells. Stained cells were analyzed by FACSVerse (BD Biosciences) or sorted using FACSARIA II (BD Biosciences) or SH800 (Sony).

Quantitative RT-PCR

Total RNA of sorted CD169⁺ and CD169[−] cells was extracted with RNeasy Micro Kit (Qiagen) or FavorPrep Total RNA Extraction Column (Favorgen) according to the manufacturer's protocol. When extracting RNA from 10,000 or fewer cells, cells were sorted directly into TRIzol LS (Thermo Fisher Scientific). Total RNA from those cells was prepared by phenol/chloroform extraction followed by purification using FavorPrep Total RNA Extraction Column. cDNA was synthesized using ReverTra Ace (TOYOBO). Quantitative RT-PCR (qRT-PCR) was performed on cDNA with THUNDERBIRD SYBR qPCR Mix (TOYOBO). Expression levels were normalized to 18S rRNA and were analyzed using the comparative threshold cycle method. The primer sequences are presented in Supplemental Table I. For the quantitation of miR expression levels, RNA was extracted with miRNeasy Mini Kit (Qiagen). TaqMan MicroRNA Assays (Applied Biosystems) were used for cDNA synthesis and qRT-PCR of miR-129 and miR-155. Snol35 served as housekeeping RNA.

DNA microarray

CD11b⁺ and/or CD11c⁺ cells of the LN and colon LP were enriched by AutoMACS Pro (Miltenyi) prior to sorting by a cell sorter to minimize the contamination of lymphocytes and epithelial cells. CD169⁺ and CD169[−] cells

were further purified by a cell sorter (FACSARIA II; BD Biosciences) based on criteria described in our previous publications (11, 17). The purity (typically 90%) of the fractionated cells was verified by flow cytometry. Total RNA extracted from FACS-purified LN cells was labeled with GeneChip Two-Cycle Target Labeling and Control Reagents (Affymetrix) and was hybridized to Affymetrix Mouse Genome 430 2.0 Array chip. From total RNA extracted from FACS-purified colon LP cells, cDNA was first amplified using Ovation RNA Amplification System V2 kit (NuGEN). The amplified cDNA was fragmented and labeled for Mouse Genome 430 2.0 GeneChip (Affymetrix) expression array analysis using FL-Ovation cDNA Biotin Module V2 kit. Total RNA extracted from LPS-stimulated BMDMs was labeled with Low-Input QuickAmp Labeling Kit (Agilent Technologies) and was hybridized to Agilent SurePrint G3 Mouse Gene Expression Microarrays using a Gene Expression Hybridization Kit (Agilent Technologies). Array raw data were digitized and further analyzed using GeneSpring software. DAVID Bioinformatics Resources 6.8 was used for an ontology analysis.

miR sequencing

The quality and concentration of the RNA was verified with the Agilent 2100 Bioanalyzer and Quantus Fluorometer (Promega), respectively. All samples showed highest RNA integrity number value of 10. Sequencing libraries were prepared according to the manufacturer's instructions for the NEBNext Multiplex Small RNA Library Prep Set for Illumina (New England BioLabs). The amplified libraries were size-selected on a BluePippin (Sage Science) using a 3% dye-free agarose cassette. The resulting purified libraries were sequenced on an Illumina HiSeq 1500 platform. After adapter trimming, the reads were mapped to the mm10 genome using Strand NGS software (version 2.9; Agilent Technologies) following small RNA analysis pipeline. After quantile normalization, significant differentially expressed miRs were identified in a scatter plot.

ELISA

IL-6, IL-10, and TNF- α concentrations were quantitated by ELISA MAX (BioLegend), according to the manufacturer's protocols. To establish CCL8 ELISA, we first generated mAbs against CCL8 by immunizing FLAG-conjugated mouse CCL8 (17) to Armenian hamsters (The Jackson Laboratory). The LN cells from those hamsters were fused with NSO bcl2 myeloma cells (25) by the PEG (Roche) method. Two clones of hybridoma cell line (clone: 2G6 and 1D5) that produce mouse CCL8-specific Ab were selected. Hamster IgG in the culture supernatant was purified by nProtein A Sepharose 4 Fast Flow (GE Healthcare). A half-area ELISA plate (Greiner) was coated with capture Ab (clone: 2G6, 5 μ g ml^{-1}) in 0.1 M sodium bicarbonate buffer (pH 9.6) for overnight at 4°C. All the following reactions were performed at room temperature. After incubation with blocking buffer (Assay Diluent [BD Biosciences] or PBS/0.2% Tween 20/5% skim milk [Yukijirushi]) for 1 h, the plate was incubated with appropriately diluted samples for 2 h. Then, the plate was incubated with biotinylated detection Ab (clone: 1D5, 0.8 μ g ml^{-1} , biotinylated in our laboratory) for 1 h followed by incubation with HRP streptavidin (BioLegend) for 30 min. Enzyme reaction was promoted by incubating the plate with TMB substrate (KPL) up to 30 min. After stopping the reaction with 2 N H₂SO₄, OD at 450 nm was measured by microplate reader (Bio-Rad).

Immunohistochemistry

Immunohistochemistry of the colon was performed as described previously, with a slight modification (17). Ten micrometer-thick frozen sections were air dried for 1 h at room temperature. Endogenous biotin was blocked using the Biotin Blocking System (Dako). The sections were further blocked with TN blocking buffer (PerkinElmer) followed by incubation with biotinylated anti-F4/80 (clone: CI:A3-1; BioLegend) and/or rabbit-IgG anti- α SMA (clone: ab5694; Abcam). The first Abs were visualized with Cy3 streptavidin (The Jackson Laboratory) and/or Alexa Fluor 488 anti-rabbit IgG (Invitrogen), respectively. For the detection of CD169, endogenous peroxidase activity was quenched with 0.5% hydrogen peroxide/methanol before the biotin blockade. The sections were incubated with biotinylated anti-CD169 (clone: M7) using TSA Biotin System (PerkinElmer). For the detection of tandem Tomato, tissue was fixed in 4% PFA/0.1 M phosphate buffer (pH 7), sequentially submerged in 10 and 20% sucrose and 50% OCT/PBS, and then snap frozen in OCT. Sections were mounted in FluorSave (Calbiochem) with DAPI (Dojindo) and observed under a fluorescent microscope (BX-X700; KEYENCE).

Immunoblotting

Five hundred thousand BMDMs were seeded in a six-well plate 48 h before lysis. Whole cell lysates were prepared using 100 μ l of RIPA buffer supplemented with protease inhibitors 5–24 h after a DEM treatment. In some experiments, BMDMs were treated with DEM in the presence of

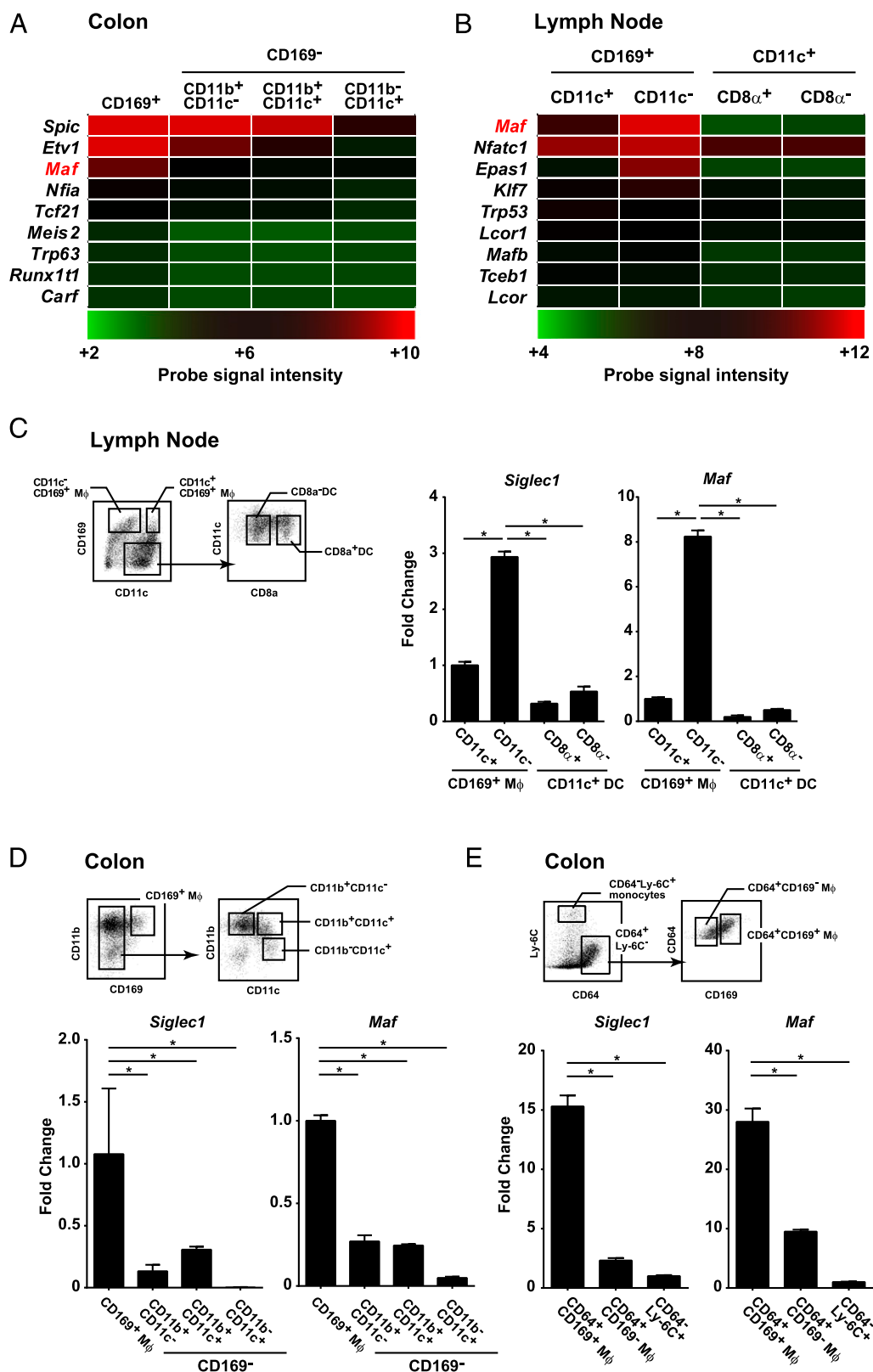


FIGURE 1. Maf is highly expressed in CD169⁺ macrophages in the colon and LNs. (**A** and **B**) Gene expression profiles of CD169⁺ and CD169⁻ cells were globally compared by microarray analysis. CD169⁺ and CD169⁻ cells were purified from the colon (**A**) and LN (**B**). Genes whose expression level showed more than 2-fold increase in CD169⁺ cells relative to CD169⁻ cells were extracted. Genes for transcription factors were further selected using the Probe Annotator tool in Reference Database of Immune Cells package. (**C–E**) The mRNA expression of indicated genes in fractionated cells was validated by qRT-PCR and was shown as fold change over doublet⁻7AAD⁻CD11b⁺CD11c⁺CD169⁺ cells in the LN (**C**), doublet⁻7AAD⁻CD11b⁺CD169⁺ cells in the colon (**D**), or doublet⁻7AAD⁻CD11b⁺CD64⁺Ly-6C⁺ monocytes in the colon (**E**). (**C–E**) Average values of PCR triplicates are shown with SD. **p* < 0.05, one-way ANOVA.

10 μ M MG132 for 5 h. The amount of protein in the whole cell lysates was quantified by BCA Protein Assay Kit (Thermo Fisher Scientific). Twenty micrograms of the lysate was resolved in a 10% SDS-PAGE and blotted using rabbit polyclonal anti-c-Maf Ab (Bethyl) and HRP-labeled anti-rabbit IgG (Dako). Chemiluminescent signal was detected by SuperSignal West Pico (Thermo Fisher Scientific). The membrane was incubated with Ab removal buffer (2% SDS, 100 mM 2-ME, 62.5 mM Tris-HCl [pH 6.8]) and reprobed using HRP-labeled anti-GAPDH Ab (MBL).

Inflammation models

For the induction of dextran sodium sulfate (DSS)-induced colitis, mice were administered 3% DSS (MW 5000; Wako Pure Chemical) in drinking water for 7 d or 2% DSS (MW 36,000–50,000; MP Biomedicals) for 5 d. Body weight was monitored daily or every other day up to 16 d after the administration of DSS. Blood samples were collected by postorbital puncture. For the induction of acetic acid-induced colitis, mice were fasted for more than 6 h and then administered with laxative by oral gavage to clean up the colon. Twelve hours later, those mice were intrarectally administered with 100 μ l of 4% acetic acid through a polytetrafluoroethylene catheter (Fuchigami, Japan). After 10 s, the acetic acid was washed out three times with 500 μ l of 0.9% normal saline. For the induction of cytoprotective/antioxidant genes in the colon macrophages, 30 μ mol/kg body weight of CDDO-Im in 200 μ l of PBS/10% DMSO/10% Chlensorphor-EL (Nacalai) was i.p. injected into mice.

Luciferase reporter assay

The murine macrophage cell line RAW264.7 or human hepatocellular carcinoma HepG2 cells were grown in DMEM/10% FBS/1% penicillin–streptomycin. Fifty thousand cells were seeded in a 24-well plate and incubated for 24 h. The cells were transfected with Maf expression plasmid (Maf-BOS-EX) and/or Nrf2 expression plasmid (Nrf2-BOS-EX) along with reporter plasmids by FuGENE6 (Promega) according to the manufacturer's protocol. The luciferase assay was performed with Dual-Luciferase Reporter Assay kit (Promega) according to the manufacturer's protocol. Twenty-four hours after the transfection, the luciferase activity was measured by a GloMax-20/20 Luminometer (Promega). Transfection efficiency was normalized to the cotransfected *Renilla* luciferase activity. HEK293T cells seeded in a 96-well plate were transfected with 100 ng of Maf 3'-UTR-psiCHECK2 plasmid along with miR mimics at a final concentration of 50 nM using Lipofectamine 3000 (Thermo Fisher Scientific) according to the manufacturer's instruction. Reporter activity was determined 24 h after the transfection. Firefly luciferase activity was used as a transfection control for *Renilla* luciferase reporter activity.

Statistical analysis

Data are presented as averages with SD or SEM. For statistical tests, Mann–Whitney *U* test was used when two groups were compared. For comparison of more than two groups, the one-way or two-way ANOVA was applied. All *p* values <0.05 were considered significant.

Data availability

The tissue macrophage microarray data reported in this paper are deposited in the Reference Database of Immune Cells (<http://refdic.rcai.riken.jp/>, accession numbers RSM00734, RSM00735, RSM01220, RSM01221, RSM12643, RSM12644, RSM12645, and RSM12646). Maf^{+/+} and Maf^{-/-} BMDM microarray data are deposited in the Gene Expression Omnibus (<https://www.ncbi.nlm.nih.gov/geo/query/acc.cgi?acc=GSE114352>, accession numbers GSE114352, GSM3140354, and GSM3140355). The miR sequencing data have been deposited in the DNA Data Bank of Japan (DDBJ, <http://ddbj.nig.ac.jp/DRASearch/>, accession numbers DRA006822, PRJDB7004, SAMD00117348–SAMD00117350, and DRX122056–DRX122058).

Results

Identification of a transcription factor highly expressed in CD169⁺ macrophages in the colon and LNs

The functional and anatomical homologies between CD169⁺ macrophages in different organs indicate a regulation of their phenotype by a common transcriptional program. By globally comparing gene expression profiles of CD169⁺ macrophages by microarray analysis, we identified the transcription factor *Maf*, which is commonly up-regulated in CD169⁺ macrophages of the colon LP and LN when compared with CD169⁻ ones (Fig. 1A, 1B). We validated the up-regulated expression of *Maf* mRNA by qRT-PCR analysis both in LN CD11c⁺CD169⁺ macrophages and in colon CD11b⁺CD169⁺ macrophages (Fig. 1C, 1D). Recently, a criterion for the clear discrimination of intestine-resident macrophages from monocytes, DCs, eosinophils, and neutrophils based on the differential expression of CD64 and Ly-6C has been proposed (26). We previously showed that the CD169⁺ macrophages are a subpopulation of intestine-resident Ly-6C^{lo}CD103⁺SiglecF⁺MHC II⁺CX3CR1⁺CD64⁺ macrophages (17). As shown in Fig. 1E, we verified that *Maf* mRNA was selectively upregulated in CD64⁺CD169⁺ macrophages in the colon. Because *Maf* is expressed also by macrophages in several other organs (Immunological Genome Project, www.immgen.org), we decided to use this transcription factor to compare the character of CD169⁺ and CD169⁻ macrophages in the colon.

Maf is dispensable for the development or localization of gut macrophages

Maf-deficient C57BL/6 fetuses die before birth owing to impaired definitive erythropoiesis in the fetal liver (27). To examine the role

Table I. Chimerism of leukocytes of Maf chimeric mice

	CD45.1 (%)			
	+/–		–/–	
	Mean	SD	Mean	SD
PB				
Neutrophil	98.4	4.2	98.0	2.7
Monocyte	98.9	2.7	97.7	3.2
T cell	93.3	3.7	99.9	0.1
B cell	99.8	0.1	99.8	0.1
BM				
Neutrophil	99.8	0.1	99.5	0.5
Monocyte	98.0	1.7	99.3	0.6
Macrophage	95.3	1.5	95.7	1.3
Eosinophil	99.0	0.8	98.5	0.4
LN				
CD11c ⁺ , CD169 ⁺ Mφ	89.3	3.8	79.0	5.1
CD11c ⁺ , CD169 ⁺ Mφ	95.8	3.1	95.6	4.6
CD11c ⁺ DC	93.8	6.6	93.0	3.3
Colon				
CD64 ⁺ , CD169 ⁺ Mφ	97.6	1.2	95.7	1.5
CD64 ⁺ , CD169 ⁻ Mφ	97.1	1.7	96.5	1.3

Numbers indicate percentage of CD45.1⁺ cells among indicated cell types 8 wk after the transplantation.

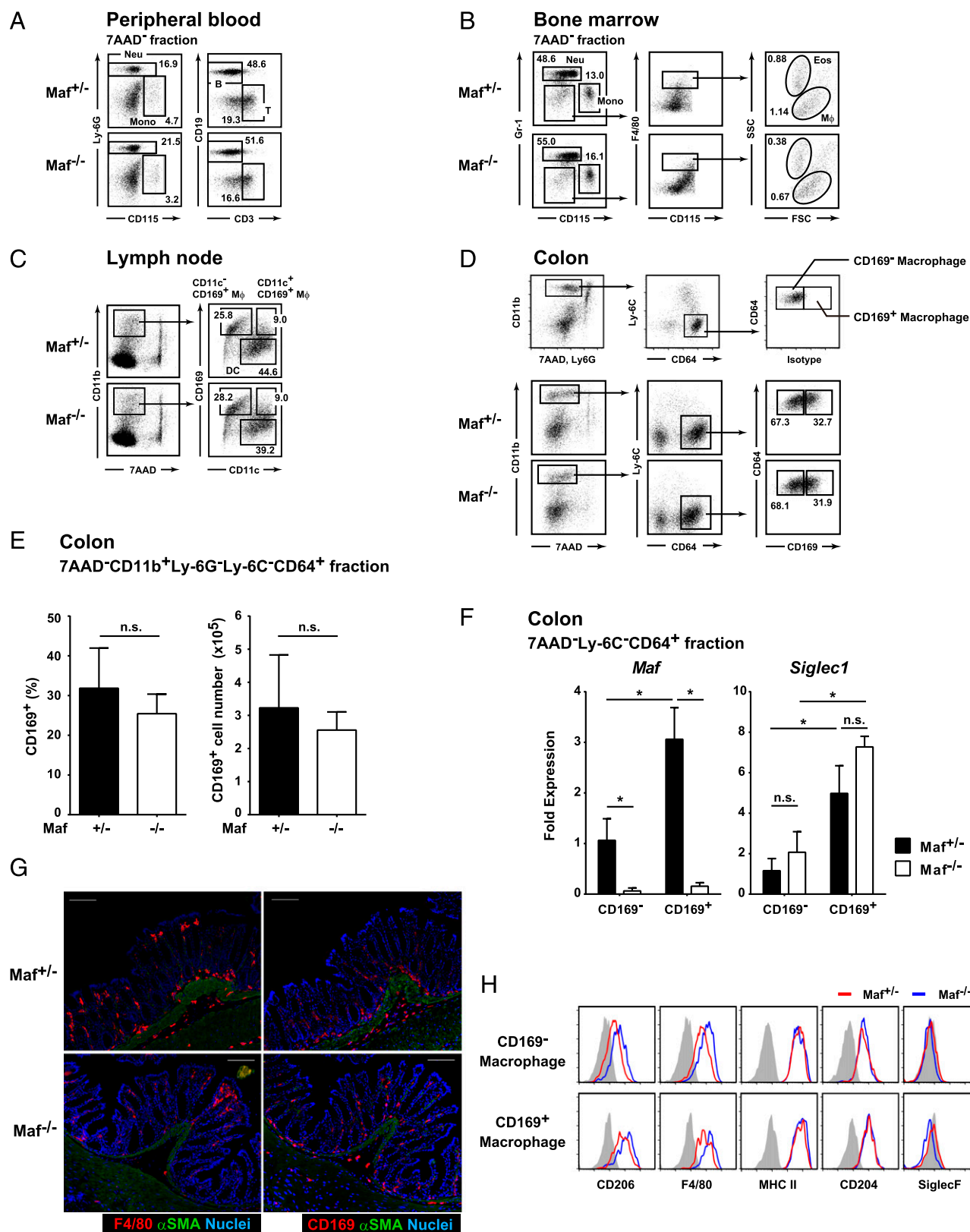


FIGURE 2. Maf deficiency does not affect the development or localization of CD169⁺ macrophages. (**A–D**) Maf deficiency does not affect the composition of immune cells. Flow cytometry of PB leukocytes (**A**), BM cells (**B**), LN cells (**C**), and colon LP cells (**D**) from Maf^{+/+} or Maf^{-/-} chimeric mice 2 mo after the transplantation. Numbers adjacent to the outlined area represent frequencies (percentages) of indicated cell types. Representative FACS profiles of eight mice (PB) or four mice (BM, LN, and colon) are shown. (**E**) Maf deficiency does not impair the expression of CD169 molecule on the colon macrophages. Frequency (percentage) and absolute number of CD169⁺ cells in the colon among 7AAD⁻CD11b⁺Ly-6G⁻Ly-6C⁻CD64⁺ fraction was determined by flow cytometry. Average values are shown with SD. $n = 3$ mice/genotype. n.s., Student t test. (**F**) Maf is not required for the expression of *Siglec1* mRNA. *Maf* and *Siglec1* mRNA level in the colon CD64^{hi}CD169⁺ or CD64^{hi}CD169⁻ macrophages from Maf^{+/+} (black bar) and Maf^{-/-} (white bar) was determined by qRT-PCR and is expressed as fold change over CD169⁻ macrophages of Maf^{+/+} mice. Average values are shown with SD. $n = 4$ mice (Maf^{+/+}) or 3 mice (Maf^{-/-}). Data are representative of two independent experiments performed in biological triplicate. (Figure legend continues)

of Maf in CD169⁺ macrophages in adult mice, we generated chimeric mice by transplanting fetal liver cells from a CD45.1⁺ Maf-deficient fetus (E13.5) into sublethally irradiated CD45.2⁺ wild-type (WT) mice or by transplanting BM cells from the primary fetal liver chimeric mice into secondary recipient mice. Two months after the transplantation, more than 95% of myeloid cells in the PB and BM were replaced by donor CD45.1⁺ cells (Table I), and the composition of immune cells in these compartments was similar between Maf^{+/-} and Maf^{-/-} chimeric mice (Fig. 2A, 2B). We also confirmed that colon-resident macrophages were almost completely replaced by CD45.1⁺ cells (Table I). Although the composition of immune cells in the LNs and colon was similar between the two genotypes of mice (Fig. 2C, 2D), chimerism (CD45.1 percentage) of CD169⁺ macrophages and DCs in LNs was relatively low at the same time point (Table I). The difference in chimerism between intestinal and LN macrophages might be attributed to the different origins of these cells (4, 28, 29). That is, the majority of tissue-resident macrophages originate from yolk sac- or fetal liver-derived progenitors that proliferate locally throughout their life independently of hematopoietic stem cells (2). In addition, radioresistant cells constantly migrate from the skin to the draining LN under both physiological and inflammatory conditions (30). In contrast, macrophages of the gut are continuously replenished by blood-borne monocytes (31, 32). Thus, we concluded that these chimeric mice were most suitable for the analysis of the roles of Maf in intestinal macrophages. We further examined the frequency and absolute number of CD169⁺ macrophages in the colon. As shown in Fig. 2D and 2E, those numbers were not statistically significant in terms of the difference between Maf^{+/-} and Maf^{-/-} chimeric mice. qRT-PCR analysis validated that the expression level of *Maf* mRNA was greatly reduced in Maf^{-/-} macrophages, whereas the *Siglec1* (CD169 coding gene) mRNA expression level in Maf^{-/-} macrophages was comparable to that in Maf^{+/-} macrophages (Fig. 2F). These findings indicate that Maf is not required for either the differentiation of or CD169 expression in intestinal macrophages. CD169⁺ macrophages show unique localization in the LP of the gut (17, 33); that is, CD169⁺ macrophages localize distantly from the epithelial border and are abundant in the area surrounding crypts. Immunohistochemistry of the colon revealed that Maf deficiency does not affect the localization of either F4/80⁺ cells (including monocytes, CD169⁺ and CD169⁻ macrophages, Fig. 2G, left) or CD169⁺ macrophages (Fig. 2G, right) in the colon. We previously reported that the colon CD169⁺ macrophages express molecules such as CD206, F4/80, and MHC II on their surface (17). FACS analysis revealed that the expression levels of those markers were similar in Maf^{+/-} and Maf^{-/-} CD169⁺ macrophages (Fig. 2H). Collectively, these findings indicate that Maf is not essential for the development, localization, and surface phenotype of the colon CD169⁺ macrophages in vivo.

Maf is essential for CCL8 production both in vitro and in vivo

In a previous study, we demonstrated the CD169⁺ macrophage-specific production of a chemokine CCL8 (17). Of note, the expression level of CCL8 in CD169⁻ cells was negligible in the

colon. Thus, we evaluated the function of Maf in CD169⁺ macrophages based on CCL8 production as an indicator. In parallel with the *Maf* expression, the *Ccl8* mRNA expression level in CD169⁺ macrophages was significantly reduced in Maf^{-/-} chimeric mice (Fig. 3A). To further examine the role of Maf in CCL8 production under inflammatory condition, we used a DSS-induced colitis model. The serum CCL8 concentration was elevated over the period of colitis in Maf^{+/-} chimeric mice (Fig. 3B). In contrast, the serum CCL8 concentration did not elevate in Maf^{-/-} chimeric mice even after the 7-d administration of DSS (Fig. 3B). These results indicate that Maf is indeed necessary for the CCL8 production in vivo.

To examine the contribution of Maf to CCL8 production more precisely in vitro, we used CD169⁺ BMDMs. We previously reported that BM cells cultured in the presence of M-CSF, but not in GM-CSF, express CD169 and CCL8 (17, 20). In good correlation with their ability to produce CCL8, BMDMs expressed a high level of *Maf*, whereas BMDCs did not (Fig. 3C). This finding suggests that Maf is required for the production of some cytokines, including CCL8, by CD169⁺ macrophages.

To directly examine the role of Maf in CCL8 production, we used BMDMs prepared from Maf^{+/-} and Maf^{-/-} chimeric mice. Maf deficiency did not impair the differentiation of BMDMs or BMDCs. In addition, the *Siglec1* mRNA expression level in Maf^{-/-} BMDMs was identical to that in Maf^{+/-} BMDMs (Fig. 3D), which is consistent with our in vivo findings (Fig. 2F). In contrast to Maf^{+/-} BMDMs, Maf^{-/-} BMDMs failed to produce CCL8 after the stimulation with LPS (Fig. 3D, 3E). Maf has been reported to regulate IL-10 production in macrophages and regulatory T cells (34, 35). In findings consistent with those of these studies, IL-10 production was found to be significantly lower in Maf^{-/-} BMDMs than in Maf^{+/-} BMDMs (Fig. 3D, 3E). Production of another cytokine, IL-6, was not impaired in Maf^{-/-} BMDMs on exposure to LPS (Fig. 3D, 3E), which thereby excludes the possibility that Maf deficiency abolishes the overall ability of cytokine production by BMDMs. These findings indicate that Maf contributes not to the differentiation of macrophages but to the regulation of the macrophage cytokine profile.

We next examined whether the forced expression of Maf was sufficient for BMDCs to produce CCL8 by transfecting BMDCs with a Maf-expressing retrovirus vector and then stimulating them with LPS. The *Maf* mRNA expression level increased by 20-fold in the Maf-transfected BMDCs when compared with empty retrovirus vector-transfected BMDCs (Fig. 3F), which exceeded the level expressed in BMDMs. BMDCs that were transfected with the Maf retrovirus vector but not with the empty retrovirus vector gained the ability to express *Ccl8* mRNA in response to LPS (600-fold over unstimulated, empty vector-transfected BMDCs, Fig. 3F). Taken together, these findings indicate that Maf is not essential for the development of CD169⁺ macrophages but plays an essential role in specifying the macrophage phenotype.

Maf promotes CCL8 expression at the transcription level

Large Maf proteins form homodimers through their leucine zipper domains and bind to consensus DNA sequences termed MAREs

n.s., **p* < 0.05, two-way ANOVA (E and F). (G) Maf deficiency does not affect the localization of the colon CD169⁺ macrophages. Immunohistochemistry analysis of the colon of indicated mice. Red, F4/80 (left); Green, CD169 (right); Blue, α smooth muscle actin (α SMA), nuclei. Original magnification $\times 20$. Scale bars, 100 μ m. Representative images of two independent experiments using different mice with similar results are shown. (H) Maf deficiency does not affect the surface expression profile of the colon CD169⁺ macrophages. Expression levels of indicated surface markers on the colon macrophages in Maf^{+/-} or Maf^{-/-} chimeric mice were examined by flow cytometry. Representative FACS plots of three different mice are shown. Eos, eosinophil; M ϕ , macrophage; Mono, monocyte; Neu, neutrophil; n.s., not significant.

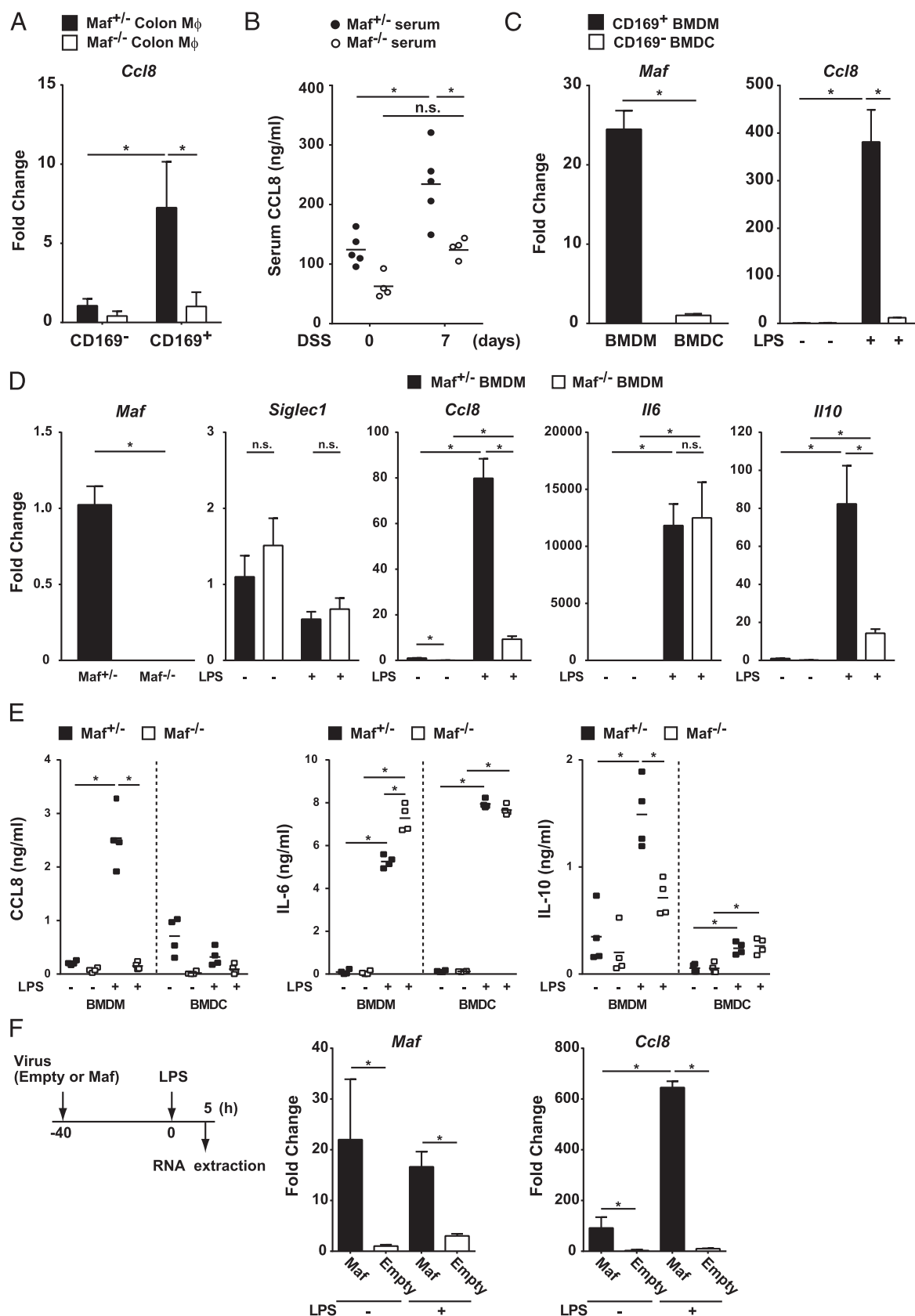


FIGURE 3. Maf is essential for the CCL8 production by macrophages. **(A)** Maf is essential for the expression of *Ccl8* mRNA. The *Ccl8* mRNA expression in CD169^{hi}CD169⁺ or CD169^{hi}CD169⁻ macrophages from *Maf*^{+/-} (black bar) and *Maf*^{-/-} (white bar) mice was determined by qRT-PCR. Expression levels are shown as fold change over CD169⁻ macrophages of *Maf*^{+/-} mice. Average values are shown with SD. $n = 4$ mice (*Maf*^{+/-}) or 3 mice (*Maf*^{-/-}). Combined data from two independent experiments are shown. $*p < 0.05$, two-way ANOVA. **(B)** Maf is essential to produce CCL8 under inflammatory conditions. Serum CCL8 concentrations at indicated time points after the DSS administration to *Maf*^{+/-} (black circle) and *Maf*^{-/-} (white circle) mice were quantitated by ELISA. Bars indicate the mean CCL8 concentration of five (*Maf*^{+/-}) or four (*Maf*^{-/-}) mice. Each symbol represents an individual mouse. n.s., $*p < 0.05$, two-way ANOVA. **(C)** The mRNA expression of *Ccl8* positively correlates with that of *Maf*. (Figure legend continues)

through a basic region (36). Maf homodimers also bind efficiently to the MARE half-site preceded by a 5'-AT-rich sequence (5'-AT-rich MARE half-site) (37). We identified three half-MARE sequences in the *Ccl8* promoter region (at -284, -204, and -152, Fig. 4). Therefore, we hypothesized that Maf could regulate CCL8 expression at the transcription level. To test this hypothesis, we transfected macrophages with the luciferase reporter plasmid containing a 333-bp fragment of the *Ccl8* promoter region (CCL8-pGL4) along with the Maf expression plasmid (Maf-BOS-EX). We chose the RAW264.7 cell line for the reporter assay because its endogenous *Maf* expression level was the lowest among available macrophage cell lines. In outcomes consistent with our hypothesis, we found that Maf enhanced *Ccl8* promoter activity in a dose-dependent manner (Fig. 4). Mutations in the MARE half-sites of the *Ccl8* promoter abolished luciferase activity (Fig. 4). These findings demonstrate that Maf promotes CCL8 expression by interacting with the MARE half-sites in the *Ccl8* promoter region.

Identification of genes under control of Maf in BMDMs

Other than CCL8, Maf has been reported to regulate IL-10, F4/80, and VCAM-1 expressions in macrophages (27, 35, 38). To characterize Maf-regulated gene clusters, we globally compared mRNA expression in LPS-stimulated *Maf*^{+/-} and *Maf*^{-/-} BMDMs by microarray analysis (Fig. 5A). The analysis revealed genes that were upregulated in *Maf*^{+/-} BMDMs, such as *Ccl8*, *Il10*, *Fgl2*, and *Mmp13* (Fig. 5B). According to ontology analysis, Maf target genes were significantly enriched for functional annotations linked to immune and inflammatory responses (Supplemental Fig. 1A). These findings suggest that Maf promotes the expression of acute inflammatory response genes in macrophages. The expression levels of conventional M1 (Supplemental Fig. 1B) and M2 (Supplemental Fig. 1C) markers were not different by a statistically significant amount between the two genotypes of macrophages, indicating that Maf determines the macrophage phenotype independently of M1 or M2 polarization.

Along with genes downregulated in *Maf*^{-/-} BMDMs, microarray analysis revealed genes that were upregulated in the absence of Maf. Among those genes, we confirmed by qRT-PCR analysis that the mRNA expression levels of three genes (*Cxcl1*, *Slpi*, and *Vegfa*) were significantly augmented in the *Maf*^{-/-} macrophages (Fig. 5C). Interestingly, these genes are implicated, whether directly or indirectly, in immune suppression (39–41) or resolution of injury (42), suggesting their roles in the late phase of inflammation. In addition to this functional similarity, two of these genes are reported to be downstream targets of Nrf2 (43–45). Nrf2 is a key transcription factor that not only promotes the expression of a wide array of antioxidants and cytoprotective proteins (46) but also suppresses macrophage inflammatory responses (47). From our results and previous reports, we speculated that Nrf2-regulated genes predominate under a Maf-suppressed condition during inflammation. To clarify this, we first examined the expression of the three above-mentioned genes in

Nrf2-deficient macrophages. As expected, the *Cxcl1*, *Slpi*, and *Vegfa* mRNA expression levels were significantly reduced in *Nrf2*^{-/-} BMDMs (Fig. 5D), suggesting the positive regulation of these genes by Nrf2 in macrophages. We next examined other Nrf2-target gene expression in Maf-deficient macrophages and found that the *Slc7a11* (xCT coding gene) mRNA expression level was higher in LPS-stimulated *Maf*^{-/-} BMDMs than in *Maf*^{+/-} BMDMs (Fig. 5E), although the *Hmox1* (HO-1 coding gene) and *Nqo1* mRNA expression levels were similar between the two genotypes of macrophages. This finding shows that Maf has the ability to downregulate some of the targets of Nrf2 in macrophages. xCT mediates resistance against oxidative stress-induced cell death (48). To determine whether up-regulated *Slc7a11* mRNA expression affects the resistance of macrophages against oxidative stress, we treated *Maf*^{+/-} and *Maf*^{-/-} BMDMs with different concentrations of tBHP, a commonly used oxidative stress inducer. Consistent with the elevated expression levels of *Slc7a11*, *Maf*^{-/-} BMDMs were more resistant to tBHP-induced cell death than *Maf*^{+/-} BMDMs 24 h after the stimulation (Fig. 5F). We further examined whether Nrf2-target genes were indeed suppressed by Maf in CD169⁺ macrophages in vivo. CDDO-Im is a small molecule that has a potent Nrf2 activation ability (49–51). We compared the *Slpi* mRNA level in CD169⁺ macrophages of *Maf*^{-/-} and *Maf*^{+/-} chimeric mice 16 h after the administration of CDDO-Im. In the absence of Maf, the *Slpi* mRNA level was upregulated in the colon CD169⁺ macrophages (Fig. 5G), indicating that Maf suppresses downstream targets of Nrf2 in tissue CD169⁺ macrophages.

Antagonistic repression of cytoprotective genes by Maf

Nrf2 interacts with the consensus sequence called the antioxidant response element (ARE), which composes a core sequence of MARE (52) (Fig. 6A). Owing to the similarity between two consensus sequences, Maf can negatively regulate ARE-mediated gene expression in human cell lines (53). To confirm that Maf represses Nrf2-target genes at the transcription level, we transfected RAW264.7 cells with the SLPI reporter plasmid (SLPI-pGL4) along with the Nrf2 and/or Maf expression plasmid. Nrf2 enhanced luciferase activity in a dose-dependent manner (Fig. 6B, left). Cotransfection of increasing the amount of Maf expression plasmid antagonized Nrf2-driven luciferase activity (Fig. 6B, left). We next transfected HepG2 cells with the xCT luciferase reporter plasmid (xCT-0.7-pGL4) containing a 0.7-kbp *Slc7a11* promoter fragment upstream of the luciferase gene (23) along with the Nrf2 and/or Maf expression plasmid. We used HepG2 cells in xCT reporter assay because high luciferase activity was detected in RAW264.7 cells not transfected with Nrf2 expression plasmid. Again, Nrf2 enhanced luciferase activity in a dose-dependent manner (Fig. 6B, right), which was inhibited by Maf (Fig. 6B, right). These findings demonstrate that Maf suppresses some of the downstream targets of Nrf2 at the transcription level.

We next determined whether Nrf2 reciprocally repress the downstream targets of Maf by quantifying the Maf-associated gene

The *Maf* and *Ccl8* mRNA expression levels in WT BMDMs (black bar) or BMDCs (white bar) were determined by qRT-PCR. Expression levels are shown as fold change over unstimulated BMDC. Average values are shown with SD. Data are representative of two independent experiments performed in biological triplicate. **p* < 0.05, Student *t* test (*Maf*) or two-way ANOVA (*Ccl8*). (D) The mRNA expression of indicated genes in *Maf*^{+/-} (black bar) and *Maf*^{-/-} (white bar) BMDMs after LPS stimulation are determined by qRT-PCR. Expression levels are shown as fold change over unstimulated *Maf*^{+/-} BMDM. **p* < 0.05, two-way ANOVA. (E) Concentrations of indicated cytokines in the culture medium of *Maf*^{+/-} (black square) and *Maf*^{-/-} (white square) BMDMs or BMDCs are quantitated by ELISA 24 h after the stimulation with LPS. (D) Average values of biological quadruplicates are shown with SD. (E) Each symbol represents a data from an individual animal. **p* < 0.05, two-way ANOVA. (F) WT BMDCs were transfected with Maf retrovirus vector or empty retrovirus vector. Forty hours after the transfection, those cells were stimulated with or without LPS for 5 h. The mRNA expression of indicated genes in those cells was quantitated by qRT-PCR and is shown as fold change over unstimulated empty retrovirus vector-transfected BMDCs. Average values are shown with SD. Representative data of two independent experiments performed in biological triplicates with similar results are shown. **p* < 0.05, two-way ANOVA. n.s., not significant.

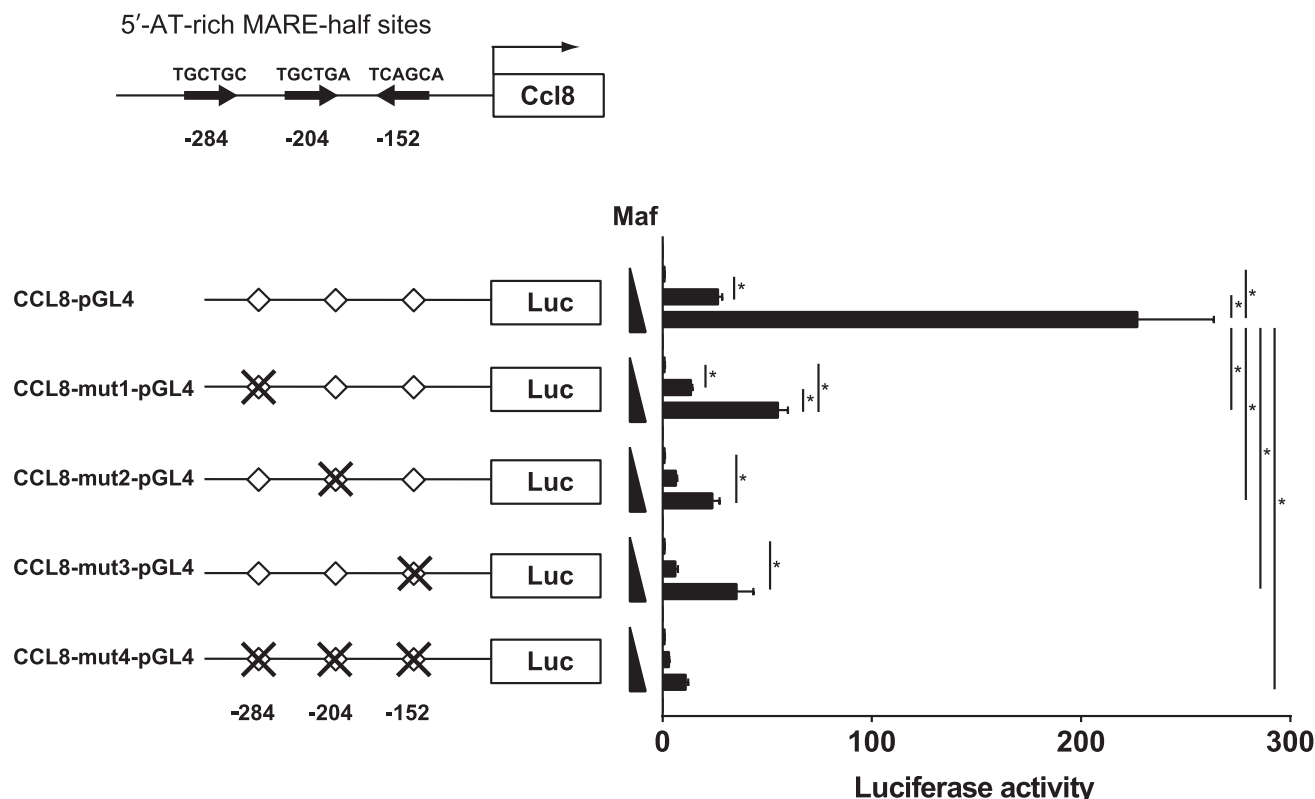


FIGURE 4. Maf promotes CCL8 expression at the transcription level. The 5'-AT-rich MARE half-sites in the *Ccl8* promoter region (top). Three hundred thirty-three-bp region from the translation start site of *Ccl8* gene that includes three MARE half-sites (-284, -204, and -152) was inserted to the luciferase reporter plasmid (CCL8-pGL4). The MARE half-sites are mutated in the mutant reporter plasmids (CCL8 mut-pGL4, bottom left). Relative luciferase activity of CCL8 reporter plasmids in the RAW264.7 cells transfected with Maf expression plasmid (bottom right). "X" represents a mutated MARE-half site. Average values are shown with SD. Representative data of two independent experiments performed in biological triplicate with similar results are shown. * $p < 0.05$, two-way ANOVA.

expression levels in BMDMs from *Nrf2*^{+/-} and *Nrf2*^{-/-} mice. DEM is an electrophilic agent that is commonly used as an oxidative stress inducer. In findings consistent with those of previous reports (23, 44, 54), we confirmed the reduced expression levels of cytoprotective/antioxidant genes (*Slpi* and *Slc7a11*) in *Nrf2*^{-/-} BMDMs after the treatment with DEM (Fig. 6C, left). However, the downstream targets of Maf (*Ccl8* and *Il10*) were not affected by the absence of *Nrf2* (Fig. 6C, right). These findings indicate that Maf antagonizes *Nrf2* transcription activity in macrophages, but not vice versa.

Macrophages change their phenotype by downregulating Maf

Because *Nrf2*-regulated antioxidative/cytoprotective responses are considered critical for tissue repair during the late phase of inflammation (55), we speculated that Maf should be downregulated under some condition in vivo that enables *Nrf2* activation in CD169⁺ macrophages. To demonstrate this, we explored for the stimulus that changes the *Maf* expression level in vitro. First, we examined the specificity of anti-c-Maf Ab by Western blotting analysis. A broad band that was observed below 50 kDa in WT but not in *Maf*^{-/-} BMDM was considered endogenous Maf (Fig. 7A, left). We found that DEM suppresses *Maf* both at mRNA expression (Fig. 7A, top right) and protein level (Fig. 7A, bottom right) in 5 h, suggesting the oxidative stress-induced downregulation of Maf in macrophages. *Maf* repression was also observed in DEM-treated, *Nrf2*-deficient BMDMs (Fig. 7B), indicating that *Nrf2* is not essential for the downregulation of Maf by oxidative stress. From these findings, we hypothesized that macrophages should change their phenotype through the downregulation of Maf. To test this hypothesis, we repressed Maf in WT BMDMs

with DEM 5 h before the stimulation with LPS and then quantified antioxidative/cytoprotective gene expression in those cells (Fig. 7C, top). As we hypothesized, pretreatment with DEM markedly suppressed the LPS-induced *Ccl8* and *Il10* expressions (Fig. 7C). In contrast, DEM pretreatment enhanced the LPS-induced expression of downstream targets of *Nrf2*, namely *Slpi* and *Slc7a11* mRNAs, by 10- and 5-fold, respectively (Fig. 7C). These findings support the concept that the oxidative stress-induced Maf repression directs macrophages to cells with the cytoprotective phenotype. To confirm that DEM-induced phenotypic conversion is dependent primarily on Maf downregulation, we transfected BMDMs with the Maf expression vector prior to the treatment with DEM. The forced expression of Maf partially cancelled the oxidative stress-induced downregulation of *Ccl8* and upregulation of *Slpi* in macrophages, suggesting the role of Maf in regulating the macrophage phenotype (Fig. 7D).

Oxidative stress accelerates Maf degradation through proteasome pathway and miR-mediated gene silencing

We then explored molecular bases that link the oxidative stress to Maf repression in macrophages. The rapid decrease in Maf protein levels indicates accelerated degradation through the proteasome pathway. To test this hypothesis, we treated BMDMs with DEM in the presence or absence of the proteasome inhibitor MG132. DEM decreased Maf at the protein level in 5 h, which was inhibited by MG132 (Fig. 7E). This result shows that DEM promotes Maf degradation through ubiquitin-proteasome pathway. We found that oxidative stress also decreases *Maf* at the mRNA level (Fig. 7A, top right), which could not be explained by degradation through the ubiquitin-proteasome pathway. It is reported that

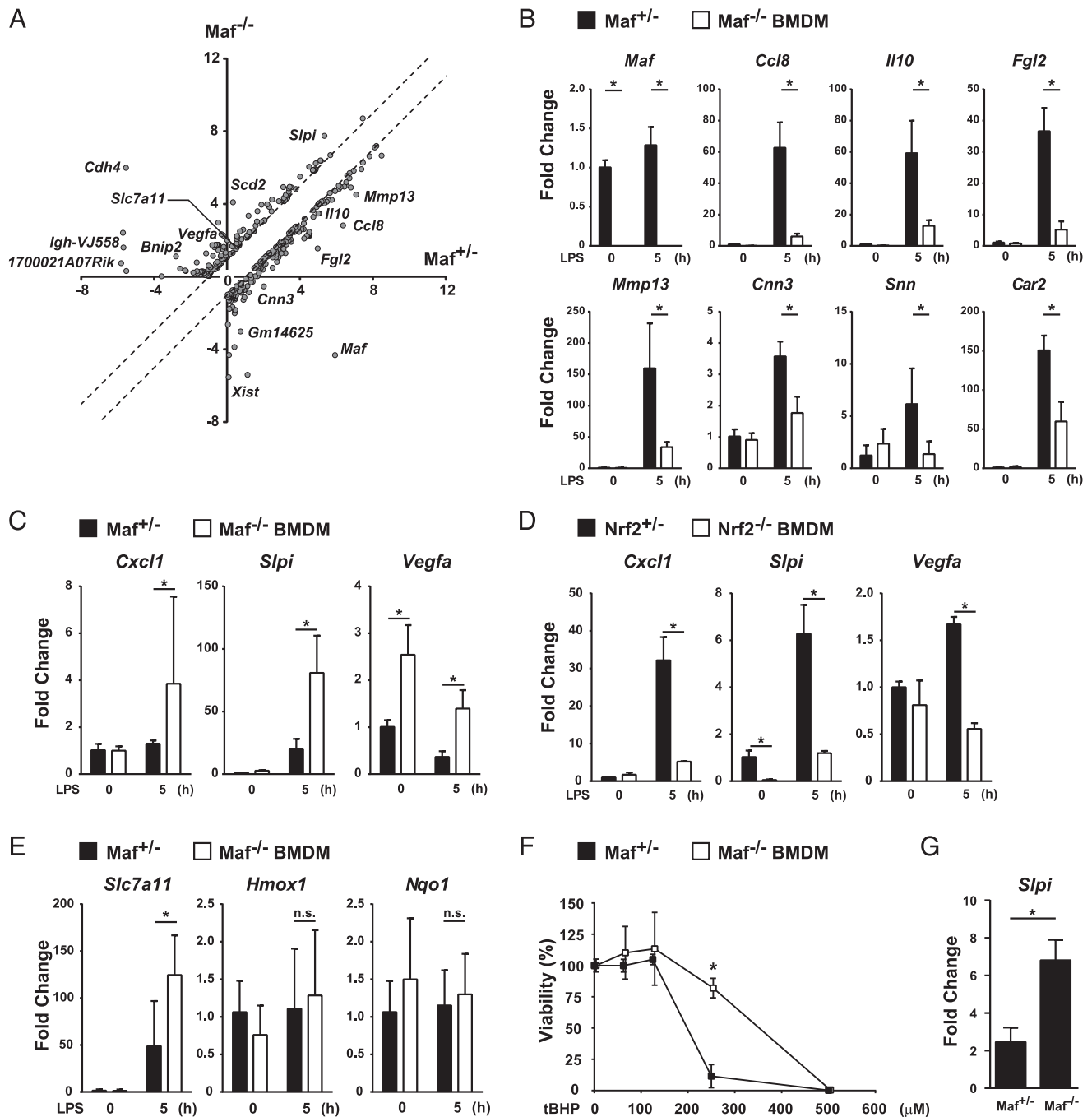


FIGURE 5. Identification of gene clusters that are regulated by *Maf* in macrophages. **(A)** Scatter plot illustrating microarray expression values in LPS-stimulated $Maf^{+/-}$ and $Maf^{-/-}$ BMDMs. Genes whose expression level showed more than 2-fold difference between the $Maf^{+/-}$ and $Maf^{-/-}$ BMDMs were extracted. **(B)** The mRNA expression of genes that are downregulated more than 2-fold in $Maf^{-/-}$ BMDMs was validated by qRT-PCR and is shown as fold change over unstimulated $Maf^{-/-}$ BMDMs. * $p < 0.05$, two-way ANOVA. **(C)** The mRNA expression of genes that was upregulated at least 2-fold in $Maf^{-/-}$ BMDMs was validated by qRT-PCR. Expression levels are shown as fold change over unstimulated $Maf^{-/-}$ BMDMs. **(B and C)** BMDMs were prepared from four different mice/genotypes, and average values of biological quadruplicate are shown with SD. * $p < 0.05$, two-way ANOVA. **(D)** Genes suppressed by *Maf* are positively regulated by *Nrf2*. The mRNA expression of indicated genes in $Nrf2^{+/-}$ and $Nrf2^{-/-}$ BMDMs 5 h after the stimulation with LPS was determined by qRT-PCR and is shown as fold change over unstimulated $Nrf2^{+/-}$ BMDMs. Average values are shown with SD. Representative data of two independent experiments performed in biological triplicate with similar results are shown. * $p < 0.05$, two-way ANOVA. **(E)** *Maf* deficiency enhances the *Slc7a11* mRNA expression. The mRNA expression of downstream targets of *Nrf2* in LPS-stimulated $Maf^{+/-}$ and $Maf^{-/-}$ BMDMs was determined by qRT-PCR and is shown as fold change over unstimulated $Maf^{+/-}$ BMDMs. BMDMs were prepared from three different mice, and average values of biological triplicate are shown with SD. * $p < 0.05$, two-way ANOVA. **(F)** $Maf^{-/-}$ BMDMs were more resistant against oxidative stress than $Maf^{+/-}$ BMDMs. Viability of BMDMs that were treated with indicated concentrations of tBHP for 24 h is plotted. Average values are shown with SD. Representative data of two independent experiments performed in biological triplicate with similar results are shown. * $p < 0.05$, two-way ANOVA. **(G)** *Maf* suppresses *Nrf2* activity in the colon CD169⁺ macrophages. The *Slpi* mRNA level in the colon CD169⁺ macrophages from $Maf^{+/-}$ or $Maf^{-/-}$ mice 16 h after administration with CDDO-Im was determined by qRT-PCR. Expression levels are shown as fold change over vehicle-injected $Maf^{+/-}$ mice. Average values of PCR triplicate are shown with SD. Combined result from two independent experiments is shown. * $p < 0.05$, two-way ANOVA. n.s., not significant.

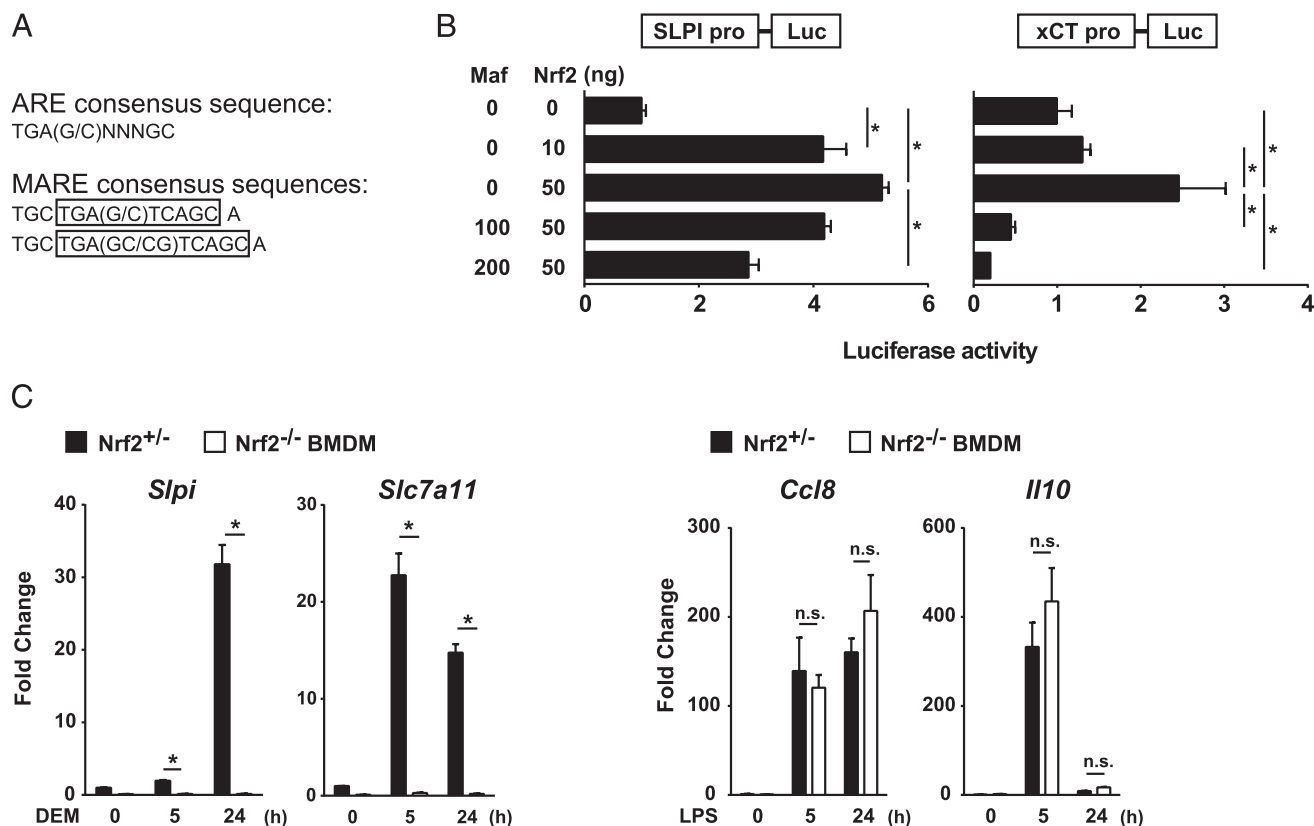


FIGURE 6. Maf inhibits Nrf2 activity at the transcriptional level. **(A)** ARE consensus sequence composes the core part of MARE consensus sequences. The boxed sequences in MARE represent ARE consensus sequence. **(B)** Maf represses downstream targets of Nrf2. RAW264.7 cells (left) or HepG2 cells (right) were transiently cotransfected with SLPI (left) or xCT (right) luciferase reporter plasmid and Nrf2 expression plasmid. Different doses of Maf expression plasmid were cotransfected to inhibit Nrf2 activity. Relative luciferase activity of reporter plasmids in the RAW264.7 cells (left) or HepG2 cells (right) is shown. $*p < 0.05$, one-way ANOVA. **(C)** Nrf2 does not suppress the mRNA expression of downstream targets of Maf. The mRNA expression of indicated genes in Nrf2^{+/+} and Nrf2^{-/-} BMDM 5 or 24 h after the stimulation with DEM (left) or with LPS (right) was determined by qRT-PCR. Expression levels are shown as fold change over unstimulated Nrf2^{+/+} BMDMs. **(B and C)** Average values are shown with SD. Representative data of two independent experiments performed in biological triplicate with similar results are shown. $*p < 0.05$, two-way ANOVA. n.s., not significant.

miR-155 is induced in macrophages during the inflammatory response (56) and that it negatively regulates *Maf* mRNA level in Th2 cells (57). Thus, we quantitated the miR-155 level in DEM-treated macrophages. Unlike TLR ligands (56), oxidative stress did not induce miR-155 expression (Supplemental Fig. 2A), thereby excluding its commitment in an oxidative stress-induced *Maf* suppression. Therefore, we globally compared miR expression levels between naive and DEM-treated BMDMs by miR sequencing analysis. The analysis revealed an upregulation of a single miR; miR-129, in DEM-treated macrophages (Fig. 7F). The enhanced miR-129 expression level in those macrophages was validated by qRT-PCR (Fig. 7G). Because there are two potential miR-129 binding sites in the *Maf* 3'-UTR (Supplemental Fig. 2B), we speculated that miR-129 has an ability to repress *Maf* mRNA. To examine whether miR-129 directly targets *Maf* mRNA, we cloned 3'-UTR of *Maf* into a luciferase reporter plasmid (57). miR-129, as well as miR-155, repressed *Maf* 3'-UTR reporter activity (Fig. 7H), suggesting their role in the repression of *Maf* mRNA. We conclude through these experiments that oxidative stress downregulates Maf in macrophages through both proteasome pathway and miR-129-mediated degradation.

The phenotypic conversion of the colon CD169⁺ macrophages by Maf in intestinal inflammation

Although we obtained evidence that Maf repression converts the macrophage phenotype in vitro, we wished to confirm such a role of Maf in the colon macrophages in intestinal inflammation. We used

DSS-induced colitis to compare the expression level of *Maf* of the colon macrophages under physiological and inflammatory condition. In accordance with our previous report, DSS administration upregulated the *Ccl8* mRNA expression level in the colon CD169⁺ macrophages in 4 d (Fig. 8A). *Maf* expression level was sustained during the acute phase of colitis. DSS removal at day 5 initiates the recovery of injured tissue. During this period, *Maf* expression level was decreased by 60% (Fig. 8A). This downregulation coincided with the decrease in *Ccl8* mRNA expression to the basal level. Notably, Nrf2 target genes (*Slpi* and *Slc7a11*) were not upregulated at the acute phase (day 4) but were progressively enhanced toward the resolution phase (day 8) of the colitis (Fig. 8A). These findings suggest an important role for *Maf* in changing the colon macrophage phenotype during different phases of intestinal inflammation. However, this model is limited in ability to assess whether the *Maf* reduction was attributable to an oxidative stress. To examine the effect of oxidative stress more directly in vivo, we induced mucosal inflammation by administering 4% acetic acid into the colon by enema. This model is useful in analyzing innate immune response in the context of oxidative stress (58). Consistent with our findings through in vitro analysis (Fig. 7A), *Maf* mRNA expression level in the colon CD169⁺ macrophages was reduced by roughly 50% (Fig. 8B). In contrast, Nrf2-target genes were enhanced by acetic acid injection (Fig. 8B). Although oxidative stress alone does not enhance *Ccl8* mRNA level in vitro (Fig. 7C), acetic acid injection upregulated *Ccl8* mRNA expression in vivo (Fig. 8B). An exposure to commensal bacteria following the disruption of mucosal barrier may have induced

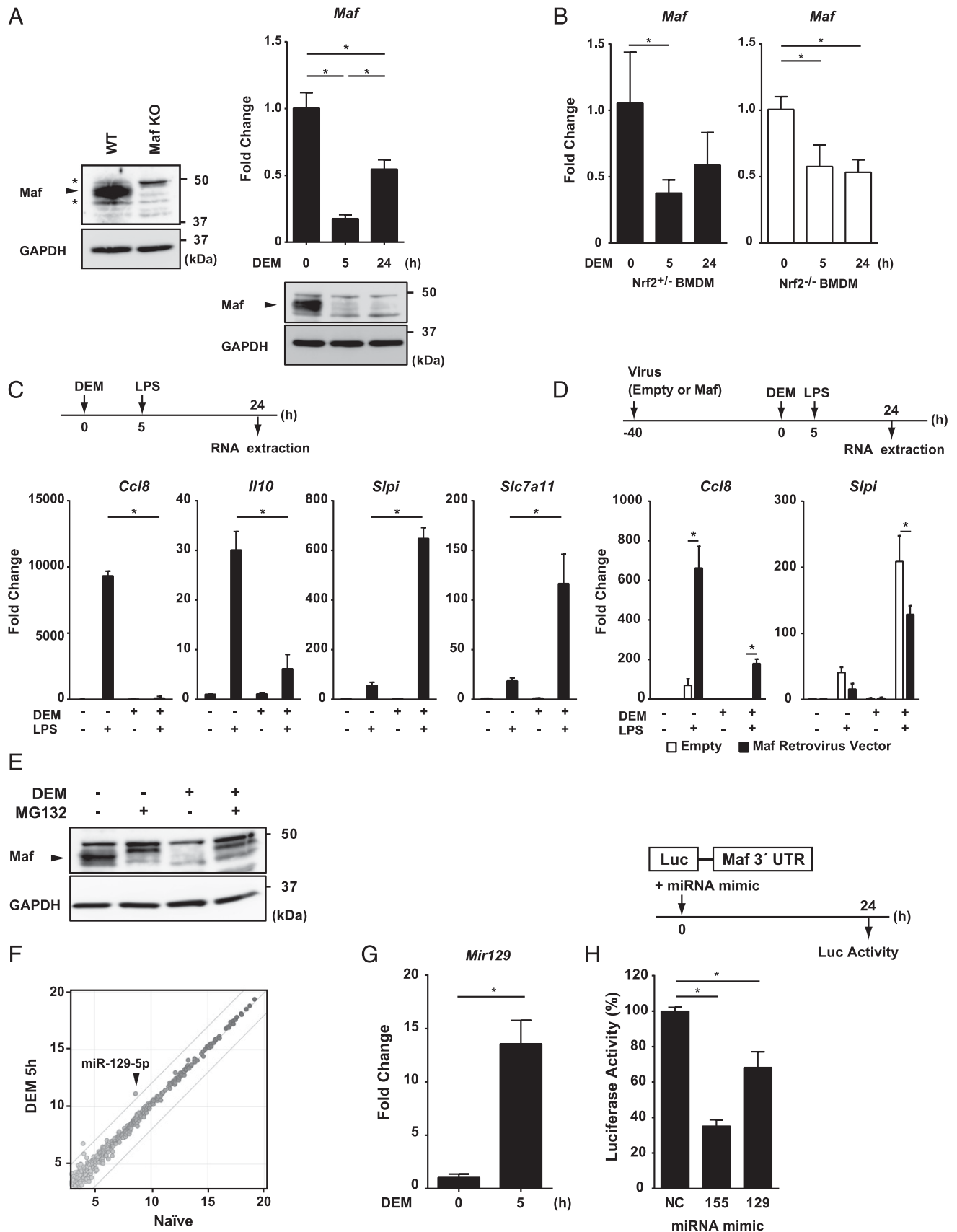


FIGURE 7. Oxidative stress downregulates Maf and switch macrophage phenotype. **(A)** Specificity of anti-c-Maf Ab was validated by Western blot (left). Arrowhead denotes endogenous Maf, and asterisks denote nonspecific bands. Electrophilic reagent DEM downregulates Maf at mRNA (top right) and protein (bottom right) levels in WT BMDMs. Average values are shown with SD. Representative data of two independent experiments performed in biological triplicate with similar results are shown. * $p < 0.05$, one-way ANOVA. **(B)** Nrf2 is not essential for the oxidative stress-induced Maf repression. Maf mRNA expression level in Nrf2^{+/-} or Nrf2^{-/-} BMDMs that were stimulated with or without DEM was quantitated by (Figure legend continues)

acute inflammatory response by CD169⁺ macrophages. Taken together, these findings show that macrophages change their phenotype by downregulating Maf activity in intestinal inflammation. Overall, these findings suggest that macrophages promote acute inflammatory response in Maf-dependent manner during the early phase of inflammation but rapidly downregulate the level of Maf, which paves the way for Nrf2-dependent cytoprotective response in the recovery phase of inflammation (Fig. 8).

Discussion

In this study, two important findings were clarified. First, we identified a transcription factor highly expressed in the colon CD169⁺ macrophages, Maf. Maf was not required for the development or localization of CD169⁺ macrophages, but it was essential for the expression of some acute inflammatory response genes, including CCL8. Second, we found that Maf not only triggers acute inflammatory responses in CD169⁺ macrophages but also represses cytoprotective/antioxidative genes. Some of those genes were downstream targets of another transcription factor, Nrf2, which is a key regulator of protection against oxidative stress. We found that acute inflammatory responses are followed by the downregulation of Maf in the colon CD169⁺ macrophages. The Maf repression converted the phenotype of those macrophages to the Nrf2-dominant, cytoprotective phenotype in vivo, which might be associated with the initiation of tissue reparative program. Collectively, our analysis provides new insights into a previously unanswered question of how macrophages initiate proinflammatory responses while retaining their tissue repairing ability.

Tissue macrophages comprise heterogeneous subsets displaying different phenotypes according to the organ in which they reside. They even switch their characteristics in adaptation to the changing environment (59), and the molecular basis that classifies different phenotypes has long been explored. Over the past two decades, macrophages have been divided into two distinct activation states, M1 and M2, on the basis of the stimuli promoting the polarization and effector cytokines that they produce as the criteria (60–63). Although the criteria contributed to the understanding of the activation states of macrophages in vitro, it is increasingly apparent that the M1–M2 dichotomy has oversimplified the complexity of macrophage differentiation in vivo (64). A new concept for macrophage differentiation relies on multistep models of activation, which integrate the environmental signals and transcriptional gene modules (64, 65). In the case of the intestines, the macrophage pool requires continual renewal from circulating monocytes (31). Under inflammatory conditions, Ly-6C^{hi} blood-borne monocytes acquire the proinflammatory phenotype by upregulating TLR2 and

NOD2 (66). In contrast, under physiological conditions, they differentiate locally into IL-10–producing anti-inflammatory intestine-resident macrophages (67). These studies indicate that the precursors of intestinal macrophages follow context-dependent fates after their entry into the tissue. However, the molecular pathway that regulates the phenotype shift of macrophages in situ was until now unexplored. We demonstrated that the “on-and-off” switching of a single transcription factor directs the conversion of gut-resident macrophages from one phenotype to another.

Maf is expressed in various cell types in a differentiation-specific manner. For example, Maf deficiency impairs the lens fiber cell differentiation (18). As we mentioned in the *Results* section, Maf in fetal liver macrophages is essential for the definitive erythropoiesis in the C57BL/6 strain (27). Another group reported that self-renewal of macrophages and embryonic stem cells requires the downregulation of two large Maf transcription factors, Maf and MafB (68, 69), indicating some important role of Maf in macrophage differentiation. In the current study, we found a novel role of Maf in changing macrophage phenotype by antagonizing Nrf2 transcriptional activity. Nrf2 plays a pivotal role in cytoprotective responses by upregulating an array of antioxidant genes. It also acts as an anti-inflammatory regulator by inhibiting proinflammatory cytokine gene transcription in macrophages (47). For example, Nrf2 deficiency exacerbates emphysema in mouse models (44). It also causes lupus-like autoimmune glomerulonephritis in mice with the ICR background (70). Thus, from the clinical viewpoint, the enhancement of Nrf2 activity appears to be an ideal therapy for a variety of chronic inflammatory diseases. We propose Maf as a novel target for the efficient activation of Nrf2; however, side effects of Maf suppression should carefully be monitored because it can inhibit beneficial acute inflammatory responses.

Among three large and three small Maf transcription factors, we focused on functions of Maf (c-Maf) that was highly expressed in the colon CD169⁺ macrophages. As MafB is known to regulate characters of macrophages in various pathological conditions (71, 72), there is a possibility that MafB also contributes to the regulation of CD169⁺ macrophages in a mechanism different from Maf.

In WT mice, the gut CD169⁺ macrophages preferentially localize toward the bottom of the villi, whereas macrophages at the villus tip do not express CD169. To address whether gut macrophages change the surface expression level of CD169 in vivo, we used a CD169 reporter system that allows fate mapping of cells that have switched on the CD169 transcription program (20). Using this system, we found that macrophages both at the tip and bottom of villi are progenies of CD169⁺ cells (Supplemental Fig. 3A). This finding suggests that under physiological conditions, monocytes gain CD169 expression during their maturation into intestine-resident

qRT-PCR and is expressed as fold change over that in unstimulated BMDM of each genotype. Average values are shown with SD. Representative data of two independent experiments performed in biological triplicate with similar results are shown. * $p < 0.05$, one-way ANOVA. (C) Repression of Maf enhances LPS-induced expression of Nrf2 target genes. WT BMDMs were pretreated with DEM or DMSO for 5 h. Those cells were stimulated with LPS or medium for the following 19 h. The mRNA expression of indicated genes was determined by qRT-PCR and is shown as fold change over unstimulated BMDMs. Average values are shown with SD. Representative results from two independent experiments performed in biological triplicate with similar results are shown. * $p < 0.05$, one-way ANOVA. (D) Phenotypic change of DEM-treated BMDMs in (C) is Maf-dependent. WT BMDMs were infected with Maf retrovirus (black bar) or empty retrovirus (white bar) vector. Forty hours later, those BMDMs were pretreated with DEM or DMSO for 5 h. Those cells were further stimulated with LPS or medium for the following 19 h. The indicated gene expression was determined by qRT-PCR and is shown as fold change over empty retrovirus-infected, unstimulated BMDMs. Average values are shown with SD. Representative data of two independent experiments performed in biological triplicate with similar results are shown. * $p < 0.05$, two-way ANOVA. (E) Oxidative stress downregulates Maf through proteasome pathway. BMDM was stimulated with DEM for 5 h in the presence or absence of MG132. Whole cell lysates were analyzed by immunoblotting with the indicated Abs. Data representative of two independent experiments are shown. (F and G) Oxidative stress induces miR-129 in macrophages. (F) miR sequencing analysis and (G) qRT-PCR analysis of BMDMs treated with or without DEM. Diagonal lines in (F) indicate 3-fold difference. Arrowhead in (F), miR-129-5p. (H) miR-129 directly suppresses *Maf* activity by binding to its 3'-UTR. *Maf* 3'-UTR reporter plasmid was cotransfected with the indicated miR mimic or negative control (NC) into HEK293T cells. Average values are shown with SD. Representative data of two independent experiments performed in triplicate with similar results are shown. * $p < 0.05$, one-way ANOVA.

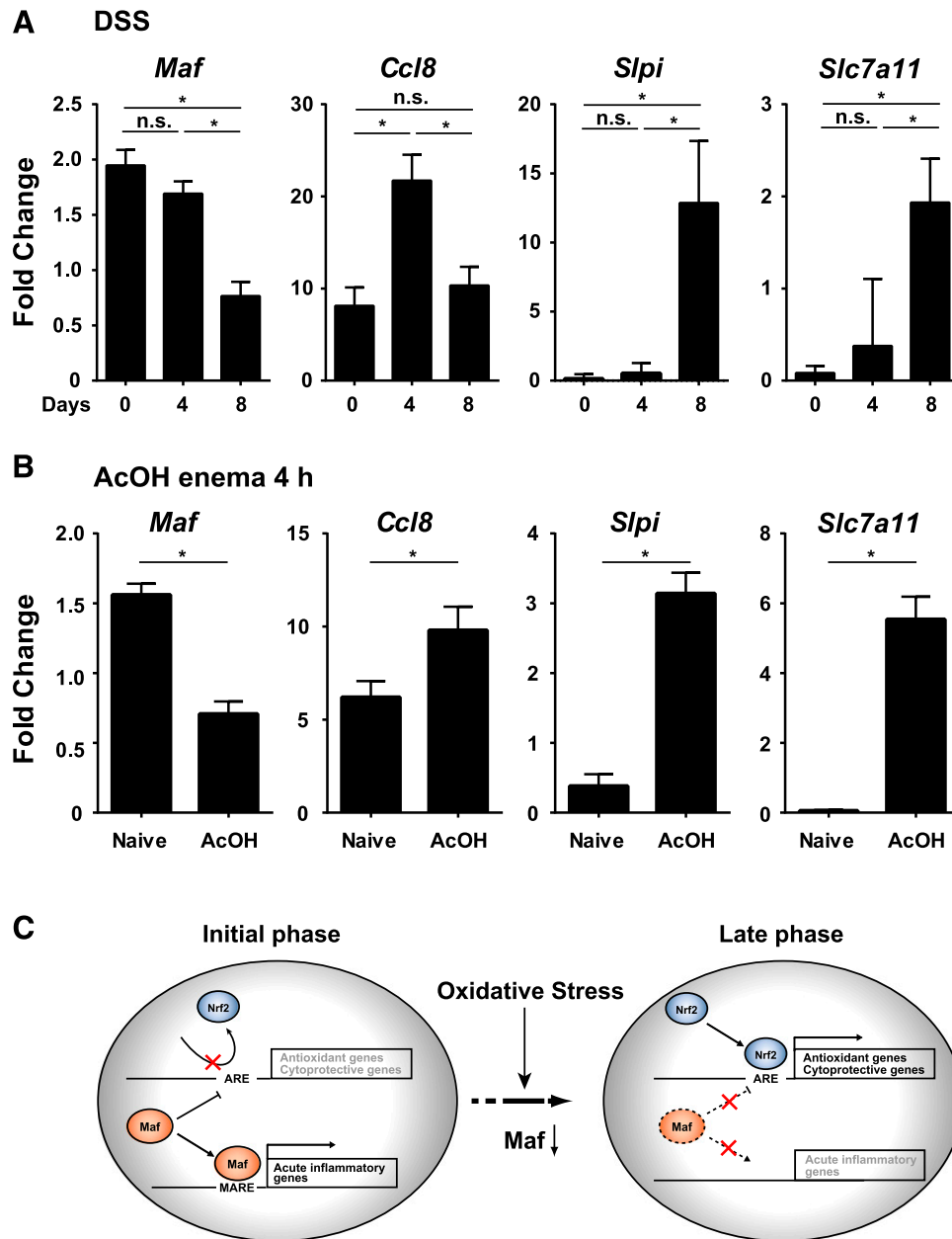


FIGURE 8. CD169⁺ macrophages in the colon dynamically change their phenotype by downregulating Maf. **(A)** CD64^{hi}CD169⁺ colon macrophages downregulate *Maf* mRNA expression and subsequently upregulate Nrf2 target genes in intestinal inflammation. The 2% DSS was administered in drinking water for 5 d. The *Maf* mRNA expression level was quantitated by qRT-PCR and is shown as fold change over naive colon CD169[−] macrophages. Average values are shown with SEM. $n = 7$ mice (day 0) or 8 mice (days 4 and 8) per group. $*p < 0.05$, one-way ANOVA. **(B)** Oxidative stress downregulates *Maf* in the colon CD64^{hi}CD169⁺ macrophages. Mucosal inflammation was induced by intrarectal administration of 4% acetic acid (AcOH). The mRNA expression of indicated genes in the colon CD64^{hi}CD169⁺ macrophages was determined by qRT-PCR and is shown as fold change over untreated colon CD169[−] macrophages. Average values are shown with SEM. $n = 8$ mice per group. $*p < 0.05$, Student t test. **(C)** Schematic model of phenotypic conversion of macrophages during different phases of inflammation. On exposure to pathogens, Maf promotes acute inflammatory response while suppressing Nrf2 activity in CD169⁺ macrophages. Oxidative stress, such as accumulation of reactive oxygen species, in the same macrophages downregulates Maf, allowing Nrf2 to promote cytoprotective gene expression. n.s., not significant.

macrophages, but some of them lose it as they approach the epithelial border. Because blood-borne monocytes do not express Maf (Fig. 1E), there might be locally supplied signal(s) that promotes Maf expression only in macrophages residing adjacent to the muscularis mucosa. Cytokines that enhance *Maf* mRNA expression in vitro, for example IL-10 (73), would be candidates that upregulate Maf in the colon.

Gut mucosa is considered one of the harshest environments in the human body because the intestine is continually exposed to a wide range of exogenous Ags. It is essential for intestinal macrophages to

maintain tolerance against those Ags to avoid uncontrolled inflammation (74, 75). Thus, the downregulation of Maf in CD169[−] macrophages residing adjacent to the epithelial border appears beneficial for both the avoidance of excess inflammatory responses and the expression of cytoprotective genes. We speculated that contact with bacterium-derived components downregulates Maf in CD169[−] macrophages. To examine this speculation, we quantitated Maf expression in the colon macrophages of mice fed under GF conditions. Contrary to our speculation, localization (Supplemental Fig. 3B) and surface CD169 (Supplemental Fig. 3C), *Siglec1*, and *Maf* mRNA

expression levels (Supplemental Fig. 3D) were identical in colon CD169⁺ macrophages isolated from specific pathogen-free and GF mice, indicating that endogenous factors other than commensal-derived components affect the Maf expression. Although we provided evidence that Maf converts the colon CD169⁺ macrophages to cells with the cytoprotective phenotype, we were unable to identify the microenvironmental signals that regulate the Maf expression level in vivo. Exploring these mechanisms is the next step to establish macrophage-targeted therapy for the treatment of inflammatory disorders.

Acknowledgments

We thank S. Nagata for pEF-BOS-EX plasmid and MGM-5 cells (GM-CSF-expressing cell line), A. Kudo for CMG14-12 cells (M-CSF-expressing cell line), and A. Miyawaki for Venus cDNA. We thank T. Suito and M. Kawana for secretarial assistance.

Disclosures

The authors have no financial conflicts of interest.

References

- Davies, L. C., S. J. Jenkins, J. E. Allen, and P. R. Taylor. 2013. Tissue-resident macrophages. *Nat. Immunol.* 14: 986–995.
- Epelman, S., K. J. Lavine, and G. J. Randolph. 2014. Origin and functions of tissue macrophages. *Immunity* 41: 21–35.
- Gordon, S., and P. R. Taylor. 2005. Monocyte and macrophage heterogeneity. *Nat. Rev. Immunol.* 5: 953–964.
- Hashimoto, D., J. Miller, and M. Merad. 2011. Dendritic cell and macrophage heterogeneity in vivo. *Immunity* 35: 323–335.
- Okabe, Y., and R. Medzhitov. 2014. Tissue-specific signals control reversible program of localization and functional polarization of macrophages. *Cell* 157: 832–844.
- Kohyama, M., W. Ise, B. T. Edelson, P. R. Wilker, K. Hildner, C. Mejia, W. A. Frazier, T. L. Murphy, and K. M. Murphy. 2009. Role for Spi-C in the development of red pulp macrophages and splenic iron homeostasis. *Nature* 457: 318–321.
- Sica, A., and A. Mantovani. 2012. Macrophage plasticity and polarization: in vivo veritas. *J. Clin. Invest.* 122: 787–795.
- Wynn, T. A., and K. M. Vannella. 2016. Macrophages in tissue repair, regeneration, and fibrosis. *Immunity* 44: 450–462.
- Ramachandran, P., A. Pellicoro, M. A. Vernon, L. Boulter, R. L. Aucott, A. Ali, S. N. Hartland, V. K. Snowden, A. Cappon, T. T. Gordon-Walker, et al. 2012. Differential Ly-6C expression identifies the recruited macrophage phenotype, which orchestrates the regression of murine liver fibrosis. *Proc. Natl. Acad. Sci. USA* 109: E3186–E3195.
- Zhang, M. Z., B. Yao, S. Yang, L. Jiang, S. Wang, X. Fan, H. Yin, K. Wong, T. Miyazawa, J. Chen, et al. 2012. CSF-1 signaling mediates recovery from acute kidney injury. *J. Clin. Invest.* 122: 4519–4532.
- Asano, K., A. Nabeyama, Y. Miyake, C. H. Qiu, A. Kurita, M. Tomura, O. Kanagawa, S. Fujii, and M. Tanaka. 2011. CD169-positive macrophages dominate antitumor immunity by crosspresenting dead cell-associated antigens. *Immunity* 34: 85–95.
- Miyake, Y., K. Asano, H. Kaise, M. Uemura, M. Nakayama, and M. Tanaka. 2007. Critical role of macrophages in the marginal zone in the suppression of immune responses to apoptotic cell-associated antigens. *J. Clin. Invest.* 117: 2268–2278.
- Ravishanker, B., R. Shinde, H. Liu, K. Chaudhary, J. Bradley, H. P. Lemos, P. Chandler, M. Tanaka, D. H. Munn, A. L. Mellor, and T. L. McGaha. 2014. Marginal zone CD169⁺ macrophages coordinate apoptotic cell-driven cellular recruitment and tolerance. *Proc. Natl. Acad. Sci. USA* 111: 4215–4220.
- Phan, T. G., J. A. Green, E. E. Gray, Y. Xu, and J. G. Cyster. 2009. Immune complex relay by subcapsular sinus macrophages and noncognate B cells drives antibody affinity maturation. *Nat. Immunol.* 10: 786–793.
- Junt, T., E. A. Moseman, M. Iannaccone, S. Massberg, P. A. Lang, M. Boes, K. Fink, S. E. Henriksson, D. M. Shayakhmetov, N. C. Di Paolo, et al. 2007. Subcapsular sinus macrophages in lymph nodes clear lymph-borne viruses and present them to antiviral B cells. *Nature* 450: 110–114.
- Martinez-Pomares, L., and S. Gordon. 2012. CD169⁺ macrophages at the crossroads of antigen presentation. *Trends Immunol.* 33: 66–70.
- Asano, K., N. Takahashi, M. Ushiki, M. Monya, A. Aihara, E. Kuboki, S. Moriyama, M. Iida, H. Kitamura, C. H. Qiu, et al. 2015. Intestinal CD169(+) macrophages initiate mucosal inflammation by secreting CCL8 that recruits inflammatory monocytes. *Nat. Commun.* 6: 7802.
- Kawauchi, S., S. Takahashi, O. Nakajima, H. Ogino, M. Morita, M. Nishizawa, K. Yasuda, and M. Yamamoto. 1999. Regulation of lens fiber cell differentiation by transcription factor c-Maf. *J. Biol. Chem.* 274: 19254–19260.
- Itoh, K., T. Chiba, S. Takahashi, T. Ishii, K. Igarashi, Y. Katoh, T. Oyake, N. Hayashi, K. Satoh, I. Hatayama, et al. 1997. An Nrf2/small Maf heterodimer mediates the induction of phase II detoxifying enzyme genes through antioxidant response elements. *Biochem. Biophys. Res. Commun.* 236: 313–322.
- Karasawa, K., K. Asano, S. Moriyama, M. Ushiki, M. Monya, M. Iida, E. Kuboki, H. Yagita, K. Uchida, K. Nitta, and M. Tanaka. 2015. Vascular-resident CD169-positive monocytes and macrophages control neutrophil accumulation in the kidney with ischemia-reperfusion injury. *J. Am. Soc. Nephrol.* 26: 896–906.
- Srinivas, S., T. Watanabe, C. S. Lin, C. M. William, Y. Tanabe, T. M. Jessell, and F. Costantini. 2001. Cre reporter strains produced by targeted insertion of EYFP and ECFP into the ROSA26 locus. *BMC Dev. Biol.* 1: 4.
- Holl, E. K. 2013. Generation of bone marrow and fetal liver chimeric mice. *Methods Mol. Biol.* 1032: 315–321.
- Sasaki, H., H. Sato, K. Kuriyama-Matsumura, K. Sato, K. Maehara, H. Wang, M. Tamba, K. Itoh, M. Yamamoto, and S. Bannai. 2002. Electrophile response element-mediated induction of the cystine/glutamate exchange transporter gene expression. *J. Biol. Chem.* 277: 44765–44771.
- Morita, S., T. Kojima, and T. Kitamura. 2000. Plat-E: an efficient and stable system for transient packaging of retroviruses. *Gene Ther.* 7: 1063–1066.
- Ray, S., and B. Diamond. 1994. Generation of a fusion partner to sample the repertoire of splenic B cells destined for apoptosis. *Proc. Natl. Acad. Sci. USA* 91: 5548–5551.
- Tamoutounour, S., S. Henri, H. Lelouard, B. de Bovis, C. de Haar, C. J. van der Woude, A. M. Woltman, Y. Reyat, D. Bonnet, D. Sichen, et al. 2012. CD64 distinguishes macrophages from dendritic cells in the gut and reveals the Th1-inducing role of mesenteric lymph node macrophages during colitis. *Eur. J. Immunol.* 42: 3150–3166.
- Kusakabe, M., K. Hasegawa, M. Hamada, M. Nakamura, T. Ohsumi, H. Suzuki, M. T. Tran, T. Kudo, K. Uchida, H. Ninomiya, et al. 2011. c-Maf plays a crucial role for the definitive erythropoiesis that accompanies erythroblastic island formation in the fetal liver. *Blood* 118: 1374–1385.
- Gordon, S., A. Plüddemann, and F. Martinez Estrada. 2014. Macrophage heterogeneity in tissues: phenotypic diversity and functions. *Immunol. Rev.* 262: 36–55.
- Hoefel, G., and F. Ginhoux. 2015. Ontogeny of tissue-resident macrophages. *Front. Immunol.* 6: 486.
- Bogunovic, M., F. Ginhoux, A. Wagers, M. Loubeau, L. M. Isola, L. Lubrano, V. Najfeld, R. G. Phelps, C. Grosskreutz, E. Scigliano, et al. 2006. Identification of a radio-resistant and cycling dermal dendritic cell population in mice and men. *J. Exp. Med.* 203: 2627–2638.
- Bain, C. C., A. Bravo-Blas, C. L. Scott, E. G. Perdiguer, F. Geissmann, S. Henri, B. Malissen, L. C. Osborne, D. Artis, and A. M. Mowat. 2014. Constant replenishment from circulating monocytes maintains the macrophage pool in the intestine of adult mice. *Nat. Immunol.* 15: 929–937.
- Yona, S., K. W. Kim, Y. Wolf, A. Mildner, D. Varol, M. Breker, D. Strauss-Ayali, S. Viukov, M. Williams, A. Misharin, et al. 2013. Fate mapping reveals origins and dynamics of monocytes and tissue macrophages under homeostasis. [Published erratum appears in 2013 *Immunity* 38: 1073–1079.] *Immunity* 38: 79–91.
- Hiemstra, I. H., M. R. Beijer, H. Veninga, K. Vrijland, E. G. Borg, B. J. Olivier, R. E. Mebius, G. Kraal, and J. M. den Haan. 2014. The identification and developmental requirements of colonic CD169⁺ macrophages. *Immunology* 142: 269–278.
- Apetoh, L., F. J. Quintana, C. Pot, N. Joller, S. Xiao, D. Kumar, E. J. Burns, D. H. Sherr, H. L. Weiner, and V. K. Kuchroo. 2010. The aryl hydrocarbon receptor interacts with c-Maf to promote the differentiation of type 1 regulatory T cells induced by IL-27. *Nat. Immunol.* 11: 854–861.
- Cao, S., J. Liu, L. Song, and X. Ma. 2005. The protooncogene c-Maf is an essential transcription factor for IL-10 gene expression in macrophages. *J. Immunol.* 174: 3484–3492.
- Kataoka, K. 2007. Multiple mechanisms and functions of maf transcription factors in the regulation of tissue-specific genes. *J. Biochem.* 141: 775–781.
- Yoshida, T., T. Ohkumo, S. Ishibashi, and K. Yasuda. 2005. The 5'-AT-rich half-site of Maf recognition element: a functional target for bZIP transcription factor Maf. *Nucleic Acids Res.* 33: 3465–3478.
- Nakamura, M., M. Hamada, K. Hasegawa, M. Kusakabe, H. Suzuki, D. R. Greaves, T. Moriguchi, T. Kudo, and S. Takahashi. 2009. c-Maf is essential for the F4/80 expression in macrophages in vivo. *Gene* 445: 66–72.
- Motz, G. T., and G. Coukos. 2011. The parallel lives of angiogenesis and immunosuppression: cancer and other tales. *Nat. Rev. Immunol.* 11: 702–711.
- Seifert, L., G. Werba, S. Tiwari, N. N. Gao, Ly, S. Allothman, D. Alqunaibit, A. Avanzi, R. Barilla, D. Daley, S. H. Greco, et al. 2016. The necrosome promotes pancreatic oncogenesis via CXCL1 and Mincle-induced immune suppression. *Nature* 532: 245–249.
- Voron, T., E. Marcheteau, S. Pernot, O. Colussi, E. Tartour, J. Taieb, and M. Terme. 2014. Control of the immune response by pro-angiogenic factors. *Front. Oncol.* 4: 70.
- Reardon, C., M. Lechmann, A. Brüstle, M. G. Gareau, N. Shuman, D. Philpott, S. F. Ziegler, and T. W. Mak. 2011. Thymic stromal lymphopoietin-induced expression of the endogenous inhibitory enzyme SLPI mediates recovery from colonic inflammation. *Immunity* 35: 223–235.
- Afonyushkin, T., O. V. Oskolkova, M. Philippova, T. J. Resink, P. Erne, B. R. Binder, and V. N. Bochkov. 2010. Oxidized phospholipids regulate expression of ATF4 and VEGF in endothelial cells via NRF2-dependent mechanism: novel point of convergence between electrophilic and unfolded protein stress pathways. *Arterioscler. Thromb. Vasc. Biol.* 30: 1007–1013.
- Ishii, Y., K. Itoh, Y. Morishima, T. Kimura, T. Kiwamoto, T. Iizuka, A. E. Hegab, T. Hosoya, A. Nomura, T. Sakamoto, et al. 2005. Transcription factor Nrf2 plays a pivotal role in protection against elastase-induced pulmonary inflammation and emphysema. *J. Immunol.* 175: 6968–6975.
- Kweider, N., A. Fragoulis, C. Rosen, U. Pecks, W. Rath, T. Pufe, and C. J. Wruck. 2011. Interplay between vascular endothelial growth factor (VEGF)

- and nuclear factor erythroid 2-related factor-2 (Nrf2): implications for pre-eclampsia. *J. Biol. Chem.* 286: 42863–42872.
46. Ishii, T., K. Itoh, S. Takahashi, H. Sato, T. Yanagawa, Y. Katoh, S. Bannai, and M. Yamamoto. 2000. Transcription factor Nrf2 coordinately regulates a group of oxidative stress-inducible genes in macrophages. *J. Biol. Chem.* 275: 16023–16029.
 47. Kobayashi, E. H., T. Suzuki, R. Funayama, T. Nagashima, M. Hayashi, H. Sekine, N. Tanaka, T. Moriguchi, H. Motohashi, K. Nakayama, and M. Yamamoto. 2016. Nrf2 suppresses macrophage inflammatory response by blocking proinflammatory cytokine transcription. *Nat. Commun.* 7: 11624.
 48. Banjac, A., T. Perisic, H. Sato, A. Seiler, S. Bannai, N. Weiss, P. Kölle, K. Tschoep, R. D. Issels, P. T. Daniel, et al. 2008. The cystine/cysteine cycle: a redox cycle regulating susceptibility versus resistance to cell death. *Oncogene* 27: 1618–1628.
 49. Keleku-Lukwete, N., M. Suzuki, A. Otsuki, K. Tsuchida, S. Katayama, M. Hayashi, E. Naganuma, T. Moriguchi, O. Tanabe, J. D. Engel, et al. 2015. Amelioration of inflammation and tissue damage in sickle cell model mice by Nrf2 activation. *Proc. Natl. Acad. Sci. USA* 112: 12169–12174.
 50. Liu, M., N. M. Reddy, E. M. Higbee, H. R. Potteti, S. Noel, L. Racusen, T. W. Kensler, M. B. Sporn, S. P. Reddy, and H. Rabb. 2014. The Nrf2 triterpenoid activator, CDDO-imidazole, protects kidneys from ischemia-reperfusion injury in mice. *Kidney Int.* 85: 134–141.
 51. Reisman, S. A., D. B. Buckley, Y. Tanaka, and C. D. Klaassen. 2009. CDDO-Im protects from acetaminophen hepatotoxicity through induction of Nrf2-dependent genes. *Toxicol. Appl. Pharmacol.* 236: 109–114.
 52. Kimura, M., T. Yamamoto, J. Zhang, K. Itoh, M. Kyo, T. Kamiya, H. Aburatani, F. Katsuoka, H. Kurokawa, T. Tanaka, et al. 2007. Molecular basis distinguishing the DNA binding profile of Nrf2-Maf heterodimer from that of Maf homodimer. *J. Biol. Chem.* 282: 33681–33690.
 53. Dhakshinamoorthy, S., and A. K. Jaiswal. 2002. c-Maf negatively regulates ARE-mediated detoxifying enzyme genes expression and anti-oxidant induction. *Oncogene* 21: 5301–5312.
 54. Habib, E., K. Linher-Melville, H. X. Lin, and G. Singh. 2015. Expression of xCT and activity of system xc(-) are regulated by NRF2 in human breast cancer cells in response to oxidative stress. *Redox Biol.* 5: 33–42.
 55. Reddy, N. M., S. R. Kleiberger, T. W. Kensler, M. Yamamoto, P. M. Hassoun, and S. P. Reddy. 2009. Disruption of Nrf2 impairs the resolution of hyperoxia-induced acute lung injury and inflammation in mice. *J. Immunol.* 182: 7264–7271.
 56. O'Connell, R. M., K. D. Taganov, M. P. Boldin, G. Cheng, and D. Baltimore. 2007. MicroRNA-155 is induced during the macrophage inflammatory response. *Proc. Natl. Acad. Sci. USA* 104: 1604–1609.
 57. Rodriguez, A., E. Vigorito, S. Clare, M. V. Warren, P. Couttet, D. R. Soond, S. van Dongen, R. J. Grocock, P. P. Das, E. A. Miska, et al. 2007. Requirement of bic/microRNA-155 for normal immune function. *Science* 316: 608–611.
 58. Millar, A. D., D. S. Rampton, C. L. Chander, A. W. Claxson, S. Blades, A. Coumbe, J. Panetta, C. J. Morris, and D. R. Blake. 1996. Evaluating the antioxidant potential of new treatments for inflammatory bowel disease using a rat model of colitis. *Gut* 39: 407–415.
 59. Stout, R. D., C. Jiang, B. Matta, I. Tietzel, S. K. Watkins, and J. Suttles. 2005. Macrophages sequentially change their functional phenotype in response to changes in microenvironmental influences. *J. Immunol.* 175: 342–349.
 60. Adams, D. O., and T. A. Hamilton. 1984. The cell biology of macrophage activation. *Annu. Rev. Immunol.* 2: 283–318.
 61. Mills, C. D., K. Kincaid, J. M. Alt, M. J. Heilman, and A. M. Hill. 2000. M-1/M-2 macrophages and the Th1/Th2 paradigm. *J. Immunol.* 164: 6166–6173.
 62. Murray, P. J., J. E. Allen, S. K. Biswas, E. A. Fisher, D. W. Gilroy, S. Goerdt, S. Gordon, J. A. Hamilton, L. B. Ivashkiv, T. Lawrence, et al. 2014. Macrophage activation and polarization: nomenclature and experimental guidelines. *Immunity* 41: 14–20.
 63. Stein, M., S. Keshav, N. Harris, and S. Gordon. 1992. Interleukin 4 potently enhances murine macrophage mannose receptor activity: a marker of alternative immunologic macrophage activation. *J. Exp. Med.* 176: 287–292.
 64. Ginhoux, F., J. L. Schultze, P. J. Murray, J. Ochando, and S. K. Biswas. 2016. New insights into the multidimensional concept of macrophage ontogeny, activation and function. *Nat. Immunol.* 17: 34–40.
 65. Okabe, Y., and R. Medzhitov. 2016. Tissue biology perspective on macrophages. *Nat. Immunol.* 17: 9–17.
 66. Zigmund, E., C. Varol, J. Farache, E. Elmaliyah, A. T. Satpathy, G. Friedlander, M. Mack, N. Shpigel, I. G. Boneca, K. M. Murphy, et al. 2012. Ly6C hi monocytes in the inflamed colon give rise to proinflammatory effector cells and migratory antigen-presenting cells. *Immunity* 37: 1076–1090.
 67. Bain, C. C., C. L. Scott, H. Uronen-Hansson, S. Gudjonsson, O. Jansson, O. Grip, M. Williams, B. Malissen, W. W. Agace, and A. M. Mowat. 2013. Resident and pro-inflammatory macrophages in the colon represent alternative context-dependent fates of the same Ly6Chi monocyte precursors. *Mucosal Immunol.* 6: 498–510.
 68. Aziz, A., E. Soucie, S. Sarrazin, and M. H. Sieweke. 2009. MafB/c-Maf deficiency enables self-renewal of differentiated functional macrophages. *Science* 326: 867–871.
 69. Soucie, E. L., Z. Weng, L. Geirsdóttir, K. Molawi, J. Maurizio, R. Fenouil, N. Mossadegh-Keller, G. Gimenez, L. VanHille, M. Beniazza, et al. 2016. Lineage-specific enhancers activate self-renewal genes in macrophages and embryonic stem cells. *Science* 351: aad5510.
 70. Yoh, K., K. Itoh, A. Enomoto, A. Hirayama, N. Yamaguchi, M. Kobayashi, N. Morito, A. Koyama, M. Yamamoto, and S. Takahashi. 2001. Nrf2-deficient female mice develop lupus-like autoimmune nephritis. *Kidney Int.* 60: 1343–1353.
 71. Hamada, M., M. Nakamura, M. T. Tran, T. Moriguchi, C. Hong, T. Ohsumi, T. T. Dinh, M. Kusakabe, M. Hattori, T. Katsumata, et al. 2014. MafB promotes atherosclerosis by inhibiting foam-cell apoptosis. *Nat. Commun.* 5: 3147.
 72. Shichita, T., M. Ito, R. Morita, K. Komai, Y. Noguchi, H. Ooboshi, R. Koshida, S. Takahashi, T. Kodama, and A. Yoshimura. 2017. MAFB prevents excess inflammation after ischemic stroke by accelerating clearance of damage signals through MSR1. *Nat. Med.* 23: 723–732.
 73. Daassi, D., M. Hamada, H. Jeon, Y. Imamura, M. T. Nhu Tran, and S. Takahashi. 2016. Differential expression patterns of MafB and c-Maf in macrophages in vivo and in vitro. *Biochem. Biophys. Res. Commun.* 473: 118–124.
 74. Ueda, Y., H. Kayama, S. G. Jeon, T. Kusu, Y. Isaka, H. Rakugi, M. Yamamoto, and K. Takeda. 2010. Commensal microbiota induce LPS hyporesponsiveness in colonic macrophages via the production of IL-10. *Int. Immunol.* 22: 953–962.
 75. Varol, C., E. Zigmund, and S. Jung. 2010. Securing the immune tightrope: mononuclear phagocytes in the intestinal lamina propria. *Nat. Rev. Immunol.* 10: 415–426.